Advanced Drug Delivery Reviews 119 (2017) 44–60

Contents lists available at ScienceDirect

Advanced Drug Delivery Reviews

journal homepage: www.elsevier.com/locate/addr

Pharmacological and physical vessel modulation strategies to improve EPR-mediated drug targeting to tumors☆

Tarun Ojha [a,b], Vertika Pathak [a], Yang Shi [a], Wim E. Hennink [b], Chrit T.W. Moonen [c], Gert Storm [b,d], Fabian Kiessling [a,*], Twan Lammers [a,b,d,*]

[a] Department of Nanomedicines and Theranostics, Institute for Experimental Molecular Imaging (ExMI), RWTH Aachen University Clinic, 52074 Aachen, Germany
[b] Department of Pharmaceutics, Utrecht Institute for Pharmaceutical Sciences (UIPS), Utrecht University, 3584 CG, Utrecht, The Netherlands
[c] Imaging division, University Medical Center Utrecht (UMCU), Utrecht, The Netherlands
[d] Department of Targeted Therapeutics, MIRA Institute for Biomedical Technology and Technical Medicine, University of Twente, 7500 AE Enschede, The Netherlands

ARTICLE INFO

Article history:
Received 1 April 2017
Received in revised form 22 June 2017
Accepted 6 July 2017
Available online 8 July 2017

Keywords:
Nanomedicine
Drug delivery
Tumor targeting
EPR
Permeabilization
Normalization
Disruption
Promotion
Hyperthermia
Radiotherapy
Sonoporation
Phototherapy

ABSTRACT

The performance of nanomedicine formulations depends on the Enhanced Permeability and Retention (EPR) effect. Prototypic nanomedicine-based drug delivery systems, such as liposomes, polymers and micelles, aim to exploit the EPR effect to accumulate at pathological sites, to thereby improve the balance between drug efficacy and toxicity. Thus far, however, tumor-targeted nanomedicines have not yet managed to achieve convincing therapeutic results, at least not in large cohorts of patients. This is likely mostly due to high inter- and intra-patient heterogeneity in EPR. Besides developing (imaging) biomarkers to monitor and predict EPR, another strategy to address this heterogeneity is the establishment of vessel modulation strategies to homogenize and improve EPR. Over the years, several pharmacological and physical co-treatments have been evaluated to improve EPR-mediated tumor targeting. These include pharmacological strategies, such as vessel permeabilization, normalization, disruption and promotion, as well as physical EPR enhancement via hyperthermia, radiotherapy, sonoporation and phototherapy. In the present manuscript, we summarize exemplary studies showing that pharmacological and physical vessel modulation strategies can be used to improve tumor-targeted drug delivery, and we discuss how these advanced combination regimens can be optimally employed to enhance the (pre-) clinical performance of tumor-targeted nanomedicines.

Contents

☆ This review is part of the *Advanced Drug Delivery Reviews* theme issue on "Emerging nanomedical solutions for angiogenesis regulation".

* Corresponding authors at: Department of Nanomedicines and Theranostics, Institute for Experimental Molecular Imaging (ExMI), RWTH Aachen University Clinic, 52074 Aachen, Germany.
E-mail addresses: fkiessling@ukaachen.de (F. Kiessling), tlammers@ukaachen.de (T. Lammers).

http://dx.doi.org/10.1016/j.addr.2017.07.007
0169-409X/

1. Introduction

Nanomedicines are employed to improve drug delivery to tumors. Upon intravenous (i.v.) administration, they circulate for prolonged periods of time and they accumulate in tumors via leaky vasculature. This pathophysiological phenomenon is known as the Enhanced Permeability and Retention (EPR) effect [1]. It is increasingly recognized, however, that the EPR effect is highly variable. Harrington and colleagues illustrated this heterogeneity in EPR-mediated tumor targeting by visualizing and quantifying the ability of ^{111}In-labeled PEGylated liposomes to accumulate in different types of patient tumors. They observed that EPR-based tumor targeting was relatively low in breast cancer, intermediate in lung cancer, and relatively high in head and neck tumors [2].

It is clear that the tumor vasculature is one of the major factors influencing the EPR effect and that each tumor (type) has different vascular characteristics, like vessel density, perfusion, maturity and pore cutoff size. The relation between tumor vascular characteristics and EPR-mediated nanomedicine accumulation was corroborated by Koukourakis et al., who studied the localization of radiolabeled PEGylated liposomal doxorubicin in patients with head and neck squamous cell carcinoma (HNSCC) and non-small cell lung cancer (NSCLC). Based on the assessment of the microvessel density (MVD) in these tumors, they concluded that the accumulation patterns in tumors correspond relatively well with MVD, with HNSCC having higher MVD and higher tumor accumulation as compared to NSCLC [3]. This notion, together with the fact that tumor blood vessels and tumor blood flow are the key contributing factors governing drug delivery to and into tumors, makes the tumor vasculature a prime target for modulating EPR-mediated tumor targeting.

The tumor vasculature has been extensively studied in the last 2–3 decades, and many efforts have been invested in pharmacological and physical strategies to enhance the EPR effect, e.g. by inducing vessel permeabilization, normalization, disruption and promotion. Via different underlying mechanisms, these strategies aim to overcome the heterogeneity in EPR and to improve nanomedicine-mediated tumor targeting (Fig. 1). Vessel permeabilization, for instance, involves the widening of endothelial pores by the use of vasomediators or external mechanical forces. Vascular normalization is an increasingly popular strategy which aims to 'correct' the structural and functional abnormalities of the tumor vasculature using low dosed antiangiogenic agents. Vessel disruption relies on the breakdown of (the integrity of) the endothelial lining by applying vascular disrupting agents or certain mechanical stimuli. Vessel promotion is the most recent vascular modulation strategy, based on enhanced angiogenesis and promotion of the vessel density in tumors, and it aims to contribute to a more uniform drug distribution. In this manuscript, we summarize the main principles of these pharmacological and physical vessel modulation strategies, provide an overview of recently published reports exemplifying their usefulness and potential, and discuss future directions to facilitate their translation into routine clinical practice.

2. Pharmacological strategies

2.1. Vascular permeabilization

Typical tumor vascular characteristics, like irregular leakiness, poor perfusion and compressed blood vessels, limit the accumulation and distribution of drugs and drug delivery systems (DDS) [4,5]. Attempts to enhance the accumulation of drugs and DDS have involved the use of inflammatory cytokines and other vasomodulators to permeabilize blood vessels and increase blood flow (Fig. 2A) [6]. Several vasomodulators, such as bradykinin, serotonin, histamine and tumor necrosis factor-alpha (TNFα), have been employed to enhance vascular permeability in tumors. However, systemic administration of these molecules can be associated with toxicity [7,8]. To overcome this problem, Eggermont and colleagues delivered TNFα, a highly potent pro-inflammatory agent, via isolated limb perfusion (ILP), and combined it with interferon-gamma and melphalan in patients with soft tissue sarcomas [9]. A strong antitumor response was observed in 87% patients, and all patients tolerated the regimen well. This combination treatment is now routinely used in the clinic for the treatment of sarcomas and melanomas [9,10]. Seki et al. reported an alternative approach, based

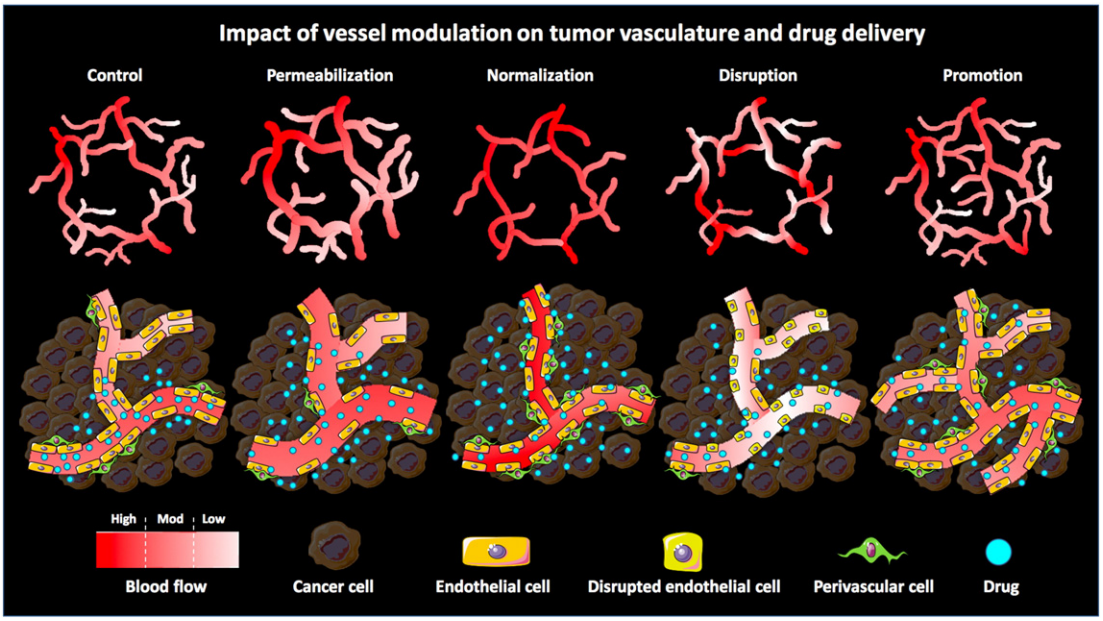

Fig. 1. Vessel modulation strategies to improve tumor-targeted drug delivery. Schematic representation of the effects of pharmacological vessel modulation strategies on the macro- and microvasculature in tumors and on tumor-targeted drug delivery. Vessel permeabilization widens the gaps between endothelial cells via vasodilation and by increasing the gaps between endothelial and perivascular cells. Vascular normalization promotes vessel maturity and improves vascular perfusion, thereby to some extent restoring the morphology and functionality of the tumor vasculature. Vessel disruption enhances vascular permeability by disrupting the endothelial lining, while at the same time reducing perfusion (particularly of immature vessels). Vessel promotion enhances the relative blood volume in tumors by increasing vessel density and distribution. Depending on the baseline vascular characteristics of tumors, different pharmacological strategies may have different effects on the accumulation and penetration of drugs and drug delivery systems.

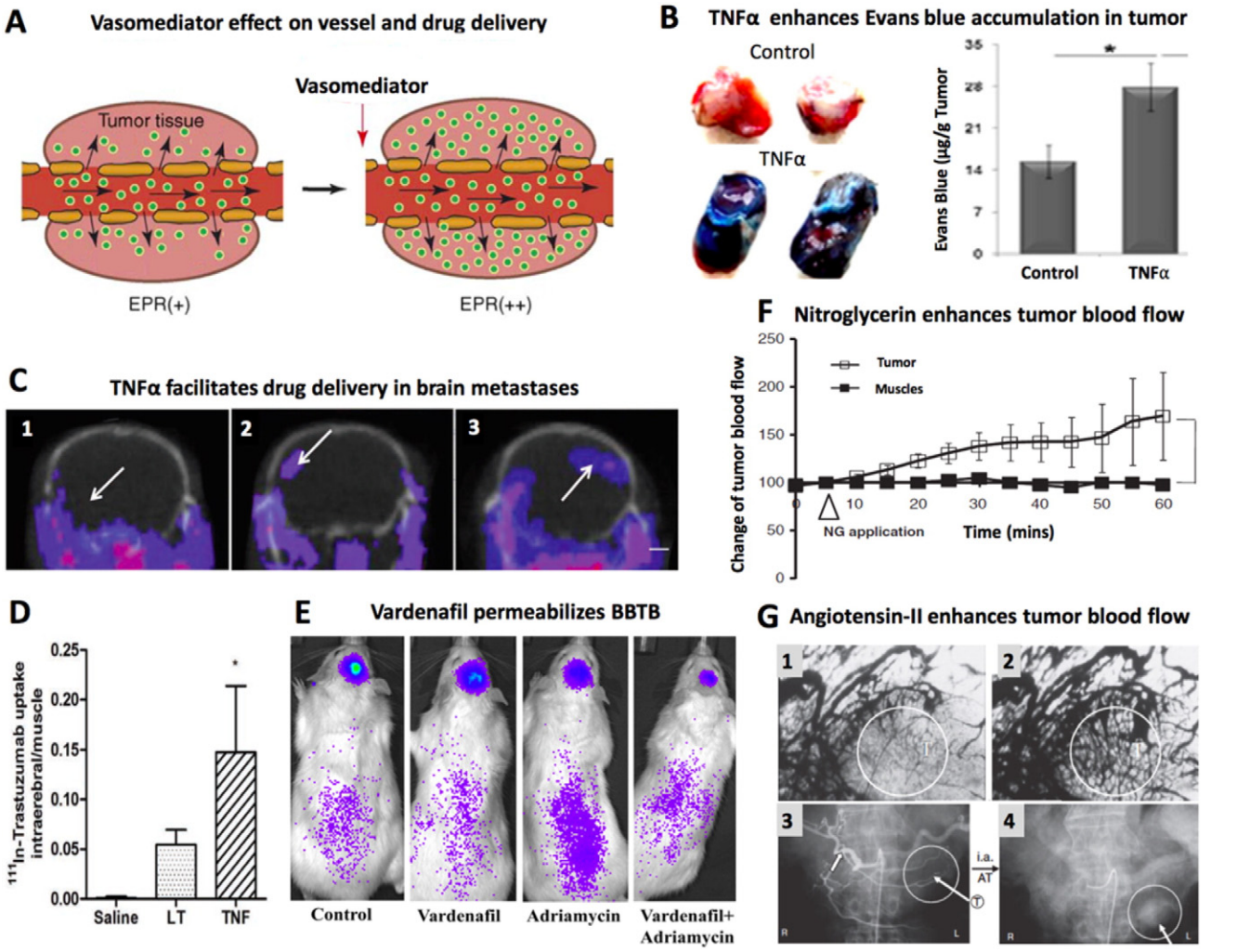

Fig. 2. Vessel permeabilization. A: Schematic representation of the effect of treatment with a vascular permeabilizing agent on drug accumulation. B: Representative mouse tumors and quantification showing massive accumulation of Evans blue dye upon pretreatment with TNFα. C: SPECT/CT images exemplifying enhanced accumulation of ^{111}In labeled trastuzumab antibodies in region affected by brain metastases upon pretreatment with TNFα. Multi panel images showing localization of radiolabeled antibody in mice treated with saline (1), lymphotoxin (LT) (2) and TNFα (3). D: Tumor/muscle uptake ratios of ^{111}In labeled trastuzumab antibodies measured by SPECT in different therapy groups. E: Bio-luminescence images demonstrating improved inhibition of brain tumor growth in rats upon combined treatment with the vasomodulator vardenafil and doxorubicin. F: Blood flow measurements after the topical application of nitroglycerin treatment on tumor and healthy muscle tissues, surprisingly shows enhanced and tumor-specific enhancement of blood flow. G: CT angiography scans of perfused blood vessels in rat (1,2) and human (3,4) tumors, exemplifying significant enhancement in blood flow after systemic treatment with angiotensin (2,4). Images are reproduced with permission from ref. [6, 11–13, 16, 18].

on the systemic administration of low dose TNFα, which is still capable to enhance vessel permeability [11]. Upon low dose TNFα treatment, they achieved an increase of 100% in the amount of Evans blue dye (EBD) accumulating in EL4 tumors (Fig. 2B).

Analogously, TNFα has also been evaluated for delivering therapeutic molecules to the brain, which is notoriously difficult, because of the presence of the blood-brain barrier (BBB). The BBB consists of closely packed endothelial cells, pericytes, astrocytes, tight junctions and extracellular matrix (ECM) components, and it severely compromises the delivery of drugs and DDS to the brain and to brain tumors. Connell et al. demonstrated TNFα-mediated selective permeabilization of the BBB at the site of cerebral metastases overexpressing TNFα receptors [12]. They intravenously administered a low dose of TNFα and lymphotoxin (LT) in mice bearing cerebral brain metastases, followed by i.v. administration of ^{111}In-labeled trastuzumab (^{111}In-BnDTPA-Tz). They observed a very high uptake of ^{111}In-BnDTPA-Tz in mice treated with TNFα (Fig. 2C–D).

As an alternative approach, the vasomodulator vardenafil (Levitra®; an inhibitor of phosphodiesterase type 5; PDE5), was employed to selectively increase blood flow and vessel permeability in 9L gliosarcoma-bearing rats [13]. Oral administration of vardenafil in PDE5-overexpressing 9L gliosarcoma significantly increased cyclic guanosine monophosphate (cGMP) levels and thereby enhanced vessel permeability. To assess the effect of vardenafil on the delivery of therapeutic molecules to 9L glioblastoma tumors, rats were treated with vardenafil and doxorubicin (Adriamycin®). Doxorubicin significantly inhibited tumor growth when combined with vardenafil, and this effect was much stronger than when both agents were given alone (Fig. 2E). Oral administration of sildenafil (Viagra®) showed similar effect on tumor blood vessels. Such combination treatments involving generally well accepted and extensively employed vessel modulators, may open up interesting new avenues to target (brain) tumors and metastases.

Nitric oxide (NO) is a well-known and potent endothelium-derived vasomodulator. It plays an important role in vascular permeability, inducing vasodilation and increasing blood flow [14,15]. Nitroglycerin (NG) is a pharmacological agent, which dilates blood vessels and increases blood flow by releasing NO, via modulating denitrase and nitrite

reductases. NG has been employed to enhance drug delivery, and works particularly well in tumors characterized by clogging problems. In this context, Seki and colleagues studied the locoregional application of NG in mice bearing sarcoma tumors [16]. They applied NG as an ointment on the skin covering the tumor (and on healthy skin tissue as a control) and subsequently measured the blood flow in malignant and healthy tissue. Ten minutes post NG application, a significant increase in blood flow was recorded in tumors, and this continued to increase until the end of experiment (Fig. 2F). Surprisingly, the blood flow remained stable in healthy skin tissue. On the other side, the topical application of NG on subcutaneous tumors increased the target site accumulation of radiolabeled polymeric drug carriers.

The use of angiotensin-II (AT-II) is an alternative approach to enhance blood flow and to promote vascular permeability in tumors, as it induces blood vessel constriction in healthy tissues and raises the systemic blood pressure. Hori et al. showed that upon slow systemic administration of AT-II, poorly perfused tumor blood vessels gradually transformed to well-perfused vessels [17]. This is exemplified by the angiographic images in Fig. 2G, which besides observations in rats, also document AT-II induced enhanced blood flow in a patient with an

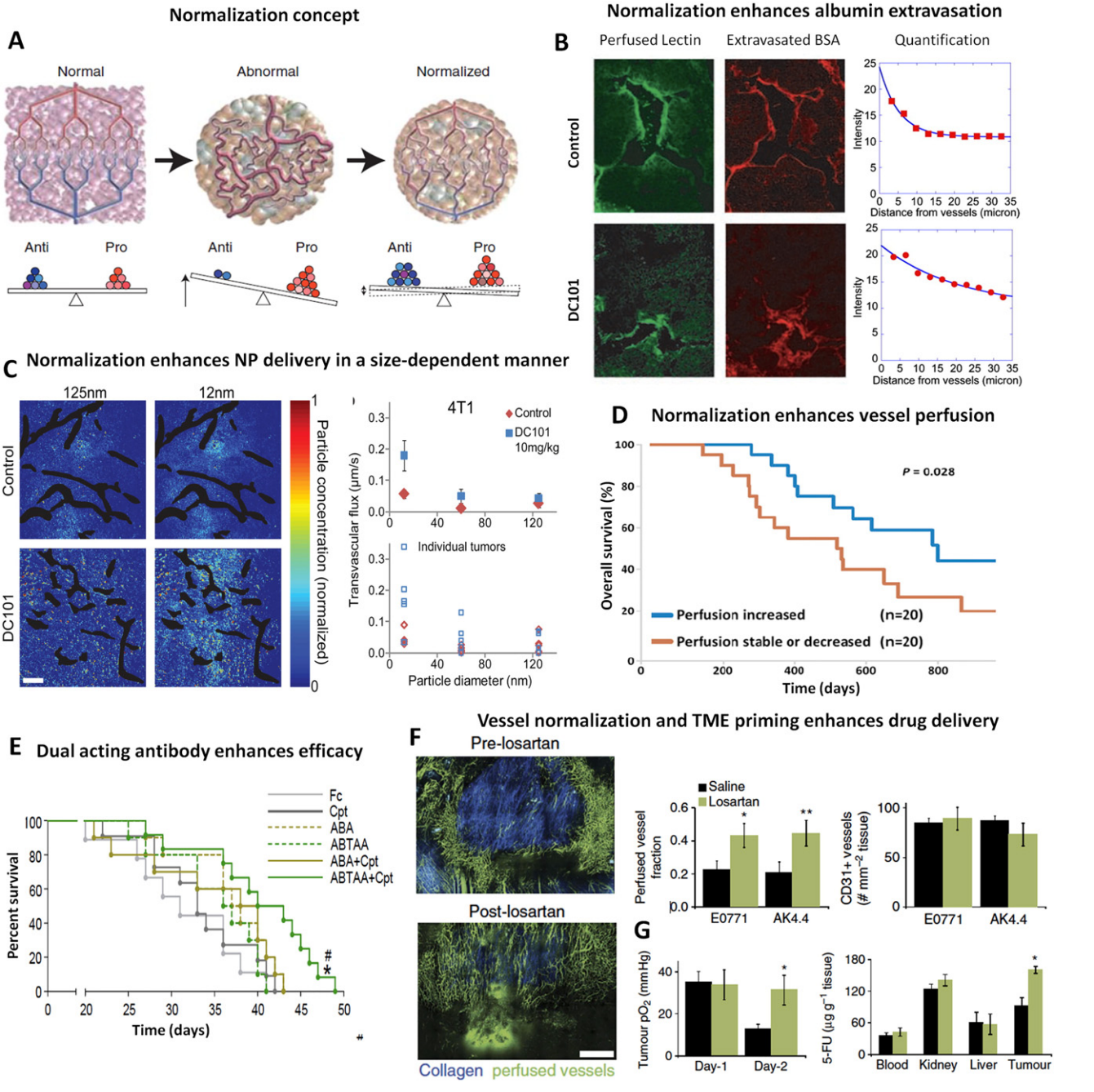

Fig. 3. Vessel normalization. A: Scheme illustrating the concept of vessel normalization. By balancing pro- and anti-angiogenic signaling, the chaotic vasculature in tumors can be structurally and functionally normalized. B: Histological analysis of frozen tumor sections showing improved extravasation and penetration of bovine serum albumin (BSA) from lectin-perfused vessels upon treatment with the VEGFR2-inhibiting antibody DC101. C: Confocal microscopy analysis, demonstrating that DC101-mediated normalization enhances the extravasation and penetration of 12 nm sized nanoparticles, but not of 125 nm sized particles. D: Kaplan–Meier survival curves of glioblastoma patients illustrating that cedinarib-based normalization treatment increases perfusion and oxygenation in 50% of patients and thereby improves the outcome of radiotherapy. E: Improved survival of mice bearing LLC tumors upon ABTAA-mediated normalization and cisplatin treatment. F–G: Intravital multiphoton microscopy images and quantification showing reduced collagen, increased perfusion in both the tumor models and enhanced oxygenation and improved drug delivery in AK4.4 tumor model upon losartan treatment. Images reproduced with permission from ref. [19, 22, 23, 25, 28, 31].

abdominal metastasis originating from liver cancer [6]. The downside of using agents such as AT-II is that they induce systemic hypertension, which may be dangerous in patients at older age, and/or suffering from co-morbidities.

Together, the above studies exemplify enhanced accumulation and improved efficacy of anticancer drugs by the use of pharmacological vessel modulators and permeabilization-promoting agents. Most studies in this regard have been done in primary tumors, and an interesting direction for the future would be to systematically study the effect of vasomodulators on the accumulation of drugs and DDS in metastases.

2.2. Vascular normalization

The vascular network in tumors is notoriously known to be chaotic, with many structural and functional irregularities, including the lack of basement membranes, abnormalities in the vessel wall and in perivascular cell morphology, and an uneven coverage of endothelial cells by perivascular cells [19–21]. Together, these abnormalities impede drug delivery and drug efficacy. One of the key reasons for these abnormalities is the imbalance between pro- and antiangiogenic factors. Restoring the balance between pro- and antiangiogenic factors might revert the tumor vasculature towards a more normal state [19]. Based on this reasoning, Rakesh Jain in 2005 proposed the concept of vascular normalization, which not only corrects structural abnormalities in the tumor vasculature but also partially restores its functionality (Fig. 3A) [19].

The initially proposed strategy to achieve vessel normalization was via inhibiting the elevated levels of vascular endothelial growth factor (VEGF) in tumors [19,20]. Indeed, Tong, Jain and colleagues managed to obtain preclinical proof-of-concept for vascular normalization by blocking VEGF signaling in tumor by administering an intermediate dose of the anti-VEGF receptor 2 (VEGFR2) antibody, DC101 [22]. In mice bearing murine breast tumor and human colon cancer, DC101 therapy remodeled the tumor vasculature by normalizing some vessels and pruning others. The treatment reduced vessel size and density, it increased vessel coverage by perivascular cells, and it partially restored the basement membrane of tumor blood vessels. Furthermore, the effect of vascular normalization on convection of (model) drug molecules from vessels into tumor tissue was validated by injecting fluorescently labeled bovine serum albumin (BSA) into mice bearing MCaIV mammary adenocarcinoma tumors. As hypothesized, histological analysis revealed higher accumulation and penetration of the model drug carrier BSA in DC101-normalized tumors as compared to control tumors (Fig. 3B).

The above study, employing BSA as an exemplary (but relatively small) drug carrier, indicates that vascular normalization may be useful to enhance EPR-mediated tumor targeting. A downside of vascular normalization, however, is that it - while normalizing the distribution and function of tumor blood vessels - may also lower vascular leakiness, thereby compromising the permeability towards larger nanocarriers, by reducing the number and size of endothelial fenestrations. Evidence in this direction has been provided by Chauhan and colleagues, showing that correcting the abnormal vasculature in murine breast tumors by blocking VEGF(R) signaling improved the delivery of albumin-based nanocarriers (~10 nm), while leaving the accumulation of larger liposomal nanomedicines unaffected (~100 nm; Fig. 3C) [23]. In line with this, when therapeutic efficacy was studied in mice bearing orthotopic E0771 mammary tumors pretreated with DC101, the antitumor efficacy of Abraxane (i.e. albumin-associated paclitaxel; ~10 nm upon reconstitution in plasma) was substantially improved, while that of Doxil (i.e. PEGylated liposomal doxorubicin; ~100 nm) was unchanged.

Early clinical trial outcomes obtained with anti-VEGF(R) agents are in line with these preclinical findings. In a pioneering trial, six patients with primary and locally advanced adenocarcinomas of the rectum were enrolled to undergo preoperative treatment with the anti-VEGF antibody bevacizumab [24]. Twelve days after bevacizumab treatment, decrease in interstitial fluid pressure (IFP), MVD and perfusion were observed, as well as increase in pericyte coverage. Normalization therapy has also already been shown to result in improved clinical outcomes when combined with radiotherapy [25]. Cediranib, a pan-VEGF receptor tyrosine kinase inhibitor, when administered to patients diagnosed with glioblastoma, improved tumor perfusion and oxygenation in 20 out of 40 patients. An overall improved survival upon radiotherapy was only observed in patients with improved perfusion and oxygen (Fig. 3D). This study shows that vascular normalization can improve therapeutic efficacy, but it also exemplifies that blocking VEGF(R) signaling only works well in certain patients. This was also observed in other clinical trials with anti-VEGF therapy [26]. In this context, it seems as if patients with high baseline vessel density are likely to respond to low dosed antiangiogenic treatment [27]. It also seems as if vascular normalization is relatively short-lived, and hard to predict (in terms of both dosing and timing), making it difficult to optimally schedule normalization therapy, and to optimally combine it with radio- and/or chemotherapy [26].

To overcome this drawback, Park et al. proposed the use of an Ang2-blocking and Tie2-activating antibody (ABTAA; which exerts dual action by blocking angiopoietin-2 (Ang2) and at the same time activating the tyrosine kinase with immunoglobulin-like and EGF-like domains 2 (Tie2)) [28]. In an orthotopic glioma model in mice, the administration of ABTAA significantly enhanced blood vessel density, pericyte coverage and vessel perfusion, and it strongly reduced RBC leakage, while ABA (i.e. an Ang2-blocking antibody) treatment alone hardly affected the tumor vasculature. Similar effects on the tumor vasculature were achieved by ABTAA in the Lewis lung carcinoma (LLC) model in mice. The potential of ABTAA was evaluated in terms of enhancing both the delivery and the efficacy of cisplatin. Compared to Fc and ABA control treatment, ABTAA significantly enhanced the accumulation of cisplatin, leading to a greater suppression of tumor growth and to an increase in overall survival (Fig. 3E). Gene expression analysis of LLC tumors treated with ABA and ABTAA revealed that pro-angiogenic expression patterns were increased in ABA-treated tumors, whereas ABTAA shifted genetic profiles from a pro-angiogenic to a vascular-stabilizing signature via Tie2 activation.

Another critical barrier affecting the accumulation and the efficacy of nanomedicines is the ECM. Even after normalizing blood vessels, the ECM can still impede the extravasation and penetration of nanomedicines [29]. ECM components like stromal cells, collagen and hyaluronan contribute to solid stress, which compresses the tumor vasculature, thereby reduces vascular perfusion. Furthermore, the ECM hinders the penetration and the distribution of extravasated nanomaterials within tumors. In order to decompress tumor blood vessels, and to enhance the penetration and distribution of nanomedicines, Jain et al. employed relaxin, a hormone which acts on the tumor microenvironment via the upregulation of matrix metalloproteinases which are responsible for collagen degradation. As expected, relaxin reduced collagen content and enhanced the tumor penetration of macromolecular agents after two weeks of treatment [30].

Extending the above approach, Chauhan et al. demonstrated the application of angiotensin inhibitor, losartan, in reducing stromal collagen and hyaluronan production [31]. After one week of losartan treatment in mice bearing E0771 breast tumors and AK4.4 pancreatic tumors, a significant drop in collagen density was observed, followed by a reduction in solid stress and less vessel compression. This resulted in enhanced vascular perfusion and increased oxygen supply (Fig. 3F–G). To assess whether the positive effect of losartan on the ECM and the vasculature improves the delivery of chemotherapeutic drugs, the concentrations of 5-FU (5-fluorouracil) were measured in tumor tissues. As hypothesized, losartan indeed improved the accumulation of 5-FU in AK4.4 tumors while not affecting accumulation in normal organs (Fig. 3G), illustrating a tumor-specific effect. The positive effect of losartan on drug delivery was confirmed in therapy studies, in two different

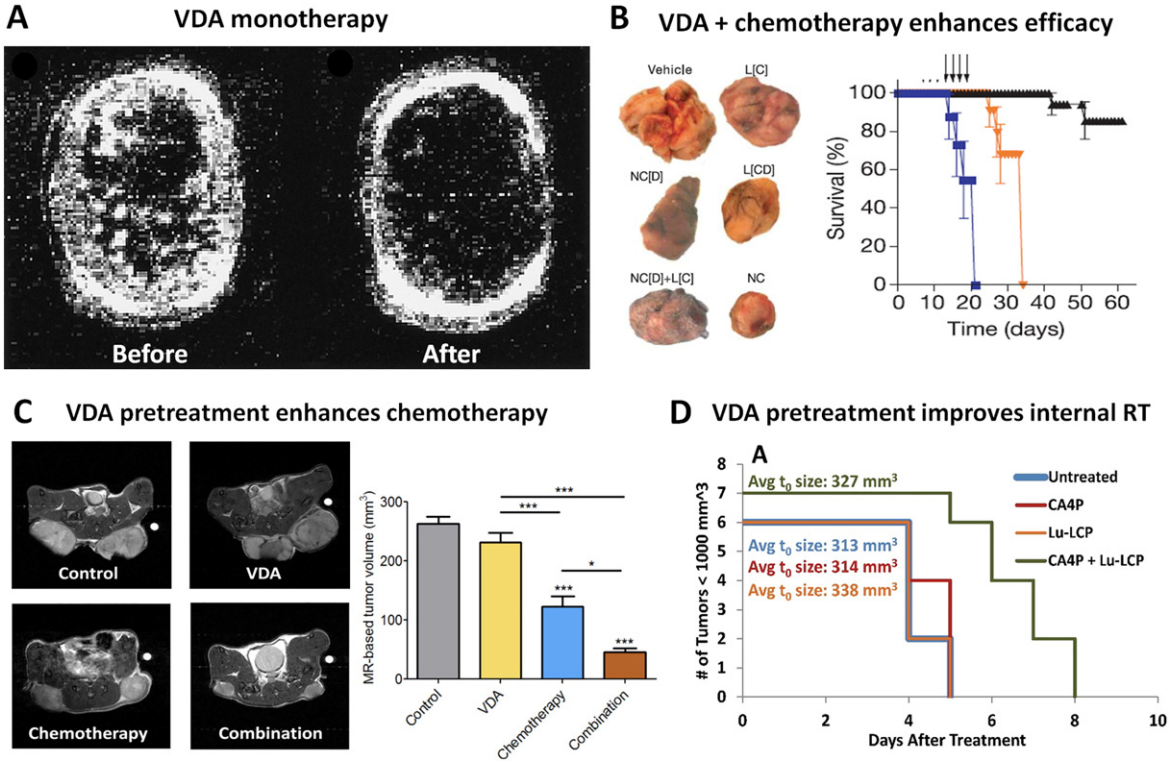

Fig. 4. Vessel disruption. A: Contrast-enhanced MRI using Gd-DTPA, illustrating the typical outcome, i.e. a necrotic core and viable rim, of treatment with vascular-disrupting agents (in this case combretastatin A4 phosphate, CA4P). B: Co-delivery of CA4P and doxorubicin by nanocells (NC) significantly reduced tumor burden as compared to other therapy groups (L[*C*]: CA4P encapsulated liposomes, NC[*D*]: nanocells containing dox only, L[*CD*]: liposomes containing both dox and CA4P, NC[*D*] + L[*C*]: co-administration of NC[*D*] and L[*C*]). Kaplan-Meier survival curves confirm the improved performance of the NC (black triangles), as compared vehicle (blue squares) and L[*CD*] (orange triangles). C: Axial T2-weighted images demonstrating significant tumor shrinkage in mice co-treated with the vascular disrupting agent DMXAA and irinotecan. D: Kaplan-Meier curves showing a significant improvement in tumor growth inhibition upon combinational therapy with CA4P and ^{177}Lu-containing lipid calcium-phosphate nanoparticles (Lu-LCP). Images are reproduced with permission from ref. [33, 37, 40, 41].

breast cancer models (E0771 and 4T1; in combination with doxorubicin), as well as in the AK4.4 pancreatic cancer model (in combination with 5-FU).

The abovementioned examples illustrate the potential of vascular normalization. However, clinical studies indicate that responses to anti-VEGF vessel normalization therapy can be highly variable. To overcome this problem, pre-selection of patients based on biomarkers and vascular imaging is proposed [25–27]. Alternative normalization treatments, based e.g. on the combined inhibition of Ang-2 and activation of Tie-2, may be useful to overcome the variability observed with anti-VEGF therapies [28,32].

2.3. Vascular disruption

Vascular disruption was initially conceived as a strategy to eradicate the tumor vasculature [33,34]. Several vascular disrupting agents (VDA) have been evaluated over the years. These for instance include combretastatin A4 phosphate (CA4P), a tubulin-binding agent which induces vessel disruption by inhibiting tubulin polymerization. Another well-known VDA is the flavonoid acetic acid-based agent 5,6-dimethylxanthenone-4-acetic acid (DMXAA), which increases NO and serotonin production, leading to endothelial damage. One of the key drawbacks with VDA monotherapy is tumor relapse due to the viable tumor rim remaining intact after therapy [33,35]. This is nicely illustrated in a study by Brindle and colleagues, in which with the help of magnetic resonance imaging (MRI), the authors visualized the viable tumor rim left after CA4P therapy in murine tumor model (Fig. 4A) [33].

To avoid tumor relapse, it was reasoned that using VDA in combination with chemo- and/or radiotherapy may have synergistic effects, as chemotherapy and radiotherapy are known to predominantly affect the tumor rim [36,37]. In this direction, Sengupta et al. developed 'nanocells', comprising of poly(lactic-*co*-glycolic) acid (PLGA) nanoparticles conjugated to doxorubicin, which were subsequently enveloped by a phospholipid *block*-copolymer membrane (Phosphatidylcholine:cholesterol:PEG-DSPE) containing CA4P [37]. The nanocells platform was designed to first release CA4P, which initially induces vessel disruption and thus create a niche for doxorubicin released from PLGA nanoparticles. They tested this platform in mice bearing B16 melanoma and Lewis lung cancer in comparison to liposomal formulations of doxorubicin and CA4P. The therapy study revealed significant tumor inhibition in both the tumor models for double-drug-loaded nanocells in comparison with all the other therapy groups, resulting in significantly improved overall survival (Fig. 4B).

The use of VDA for enhancing drug delivery became prominent after Tozer et al. reported - using intravital microscopy - a rapid increase in vascular permeability to albumin immediately after the administration of CA4P in rats bearing P22 carcinosarcoma [38]. This finding was corroborated by Baguley et al. using DMXAA [39]. They studied the extravasation of EBD in C-38 adenocarcinoma upon administration of DMXAA in wild type vs. TNFα receptor-1 (TNFR1) and TNFα knockout mice. They reported a significantly enhanced extravasation of EBD in tumors in wild type mice, at all doses of DMXAA, while less extravasation was observed in both knockout models. Based on these findings, they proposed that DMXAA enhances vessel permeability by inducing endothelial cell apoptosis. The fact that less extravasation was observed in both knockout models indicates that TNFα plays an important role in the antivascular response to DMXAA.

These initial proof-of-principle studies stimulated further exploration of the potential of VDA for enhancing the delivery of drugs and DDS. In this regard, Folaron et al. investigated the potential of DMXAA

in combination with chemotherapy in a human HNSCC xenograft model [40]. They found that pre-administration of DMXAA enhanced the anticancer activity of irinotecan, showing significant tumor growth inhibition compared to VDA or irinotecan alone, which was validated using MRI (Fig. 4C). Similar results were achieved in combination with docetaxel [40].

Extending these findings, Satterlee and colleagues studied the effect of CA4P pretreatment on the accumulation and efficacy of radioisotope-loaded nanoparticles in three different tumor models [41]. CA4P pretreatment in mice bearing subcutaneous UMUC3/3T3 ovarian tumor and orthotopic 4T1 breast tumors resulted in significantly higher levels of accumulation of ^{177}lutetium-loaded lipid calcium-phosphate nanoparticles (^{177}Lu-LCP) compared to non-pretreated mice. However, in the case of B16 melanoma tumors, CA4P pretreatment did not significantly enhance ^{177}Lu-LCP accumulation, likely due to high baseline levels of EPR in B16 tumors. They next studied the effect of CA4P pretreatment on the retention time of ^{177}Lu-LCP in UMUC3/3T3 tumors. Combination therapy of CA4P and ^{177}Lu-LCP significantly inhibited tumor growth in comparison to CA4P and ^{177}Lu-LCP treatment alone (Fig. 4D). In addition, at the time each tumor reached 1000 mm^3, the accumulation of ^{177}Lu-LCP was significantly higher in CA4P-pretreated tumors than in tumors treated with ^{177}Lu-LCP alone. This study demonstrates that CA4P pretreatment can help to enhance the accumulation, retention and efficacy of ^{177}Lu-LCP nanoparticles.

The above mentioned studies demonstrate the potential of vessel disruption for enhancing the target site accumulation of anticancer agents. However, since the systemic administration of VDA is typically associated with quite severe side effects, further efforts are needed to make this therapeutic strategy suitable for use in the clinic [42].

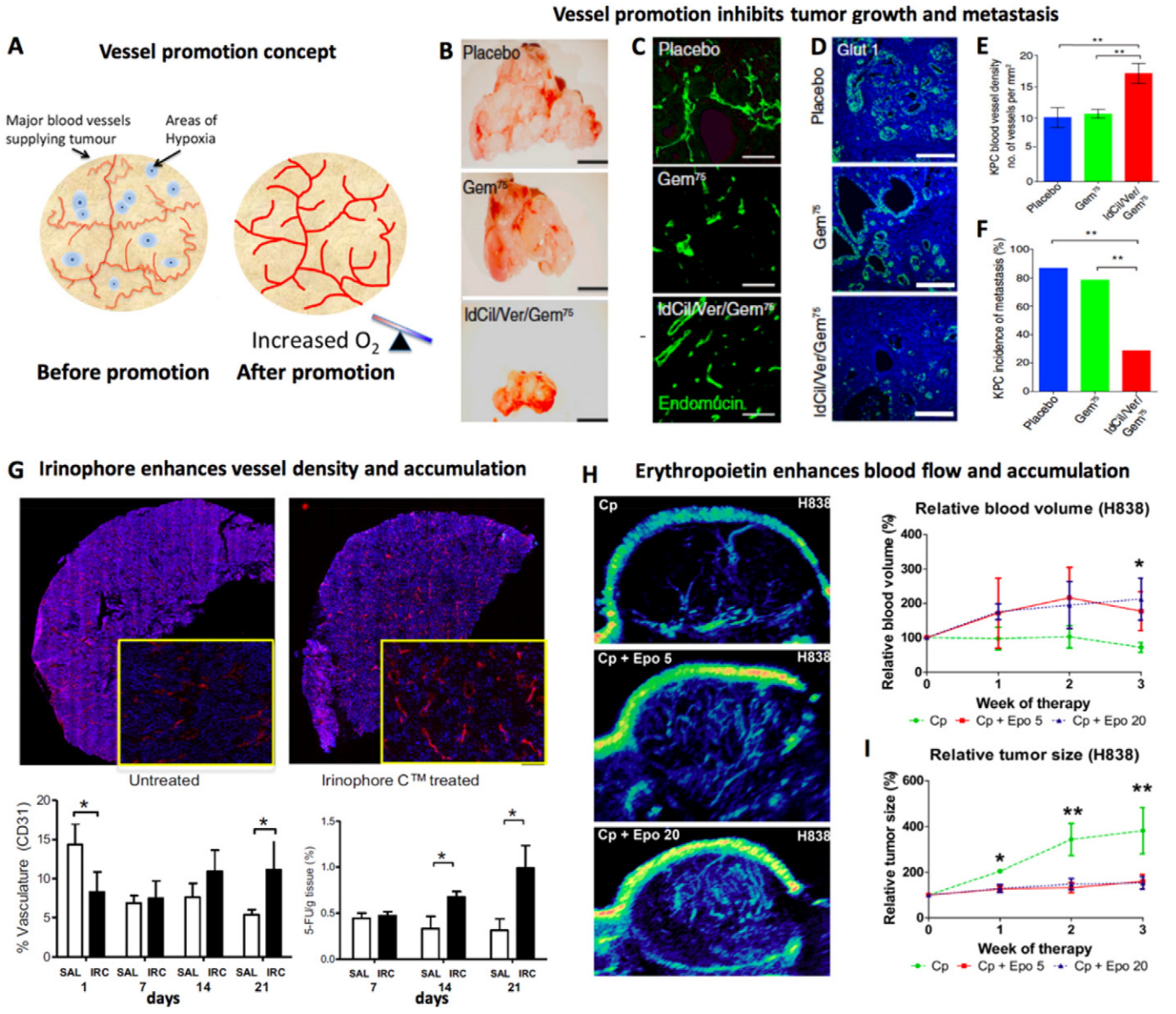

Fig. 5. Vessel promotion. A: Schematic figure illustrating the concept of vessel promotion. B: Representative images of spontaneous pancreatic tumors in KPC mice exemplifying strong antitumor efficacy upon combining gemcitabine with verapamil and cilengitide. C: Endomucin staining showing significant increase in vessel coverage upon IdCil/Ver/Gem treatment. D: Glut-1 staining showing significant decrease in hypoxia upon IdCil/Ver/Gem treatment. E: Quantification of endomucin staining, confirming vessel promotion. F: Significant decrease in the number of metastases in mice treated with IdCil/Ver/Gem G: Histological images of tumor sections stained with CD31 and DAPI, showing increased CD31$^+$ vessel density upon prolonged Irinophore C™ treatment, resulting in a significant increase in 5-FU accumulation. H: Maximum intensity over time ultrasound imaging illustrating increased perfusion and higher relative blood volume in tumors treated with erythropoietin (Epo). I: Erythropoietin-mediated vessel promotion potentiates the antitumor effect of carboplatin. Images reproduced with permission from ref. [46–49].

2.4. Vascular promotion

Vascular promotion is the most recently developed vessel modulation strategy. It aims to address the problems related to poor intratumoral drug accumulation and distribution by increasing vessel density and improving perfusion (Fig. 5A). At first glance, this concept may seem somewhat paradoxal, given the fact that enhanced angiogenesis promotes tumor growth [43–45]. The latter notion has led to the use of low dosed antiangiogenic therapy to induce vascular normalization (see above, Section 2.2). However, also moderately induced angiogenesis or vascular promotion may be useful to achieve improved accumulation, more homogeneous distribution and enhanced efficacy of anticancer agents, at least in some tumor models.

Hodivala-Dilke and colleagues pioneered the vessel promotion strategy and provided the first preclinical proof-of-concept for the potential of this approach [46]. They demonstrated that a low dose of the antiangiogenic agent cilengitide (IdCil), when combined with the calcium channel blocker verapamil (Ver), led to enhanced angiogenesis, resulting in increased vessel density, vessel dilation and blood flow. Together, these effects enhanced the tumor accumulation of the nucleoside analogue gemcitabine (Gem). They went on to test the therapeutic efficacy of this multi-drug cocktail (i.e. IdCil + Ver + Gem) in well-vascularized LLC and A549 xenografts, as well as in spontaneously developing and poorly vascularized KPC mouse pancreatic tumors. The triple combination therapy significantly reduced LLC tumor burden. In mice with A549 lung cancer metastases, IdCil with or without Ver + Gem increased vessel density and perfusion, and the combination of IdCil + Ver + Gem decreased the number of metastatic nodules. Similarly, IdCil + Ver + Gem significantly reduced KPC pancreatic tumor burden compared to gemcitabine alone (Fig. 5B). Histological analysis of excised tumors showed increased vessel density and reduced hypoxia in tumors treated with IdCil + Ver + Gem, while vessel density and hypoxia levels in gemcitabine-treated tumors were identical to those of untreated controls (Fig. 5C–E). Moreover, the number of metastases was significantly lower in mice treated with IdCil + Ver + Gem, whereas treatment with gemcitabine alone did not affect the number of metastases (Fig. 5F).

Findings going in a similar direction were reported by Neijzen et al., who pretreated mice bearing colon cancer-based patient-derived xenografts first with liposomal Irinotecan (IrC™) and then with 5-FU [47]. Histological analysis based on CD31 staining showed that pretreatment with IrC™ initially reduced the microvessel density. However, after multiple IrC™ treatments, a significant increase in microvessel density was observed. This was paralleled by enhanced vessel perfusion, and

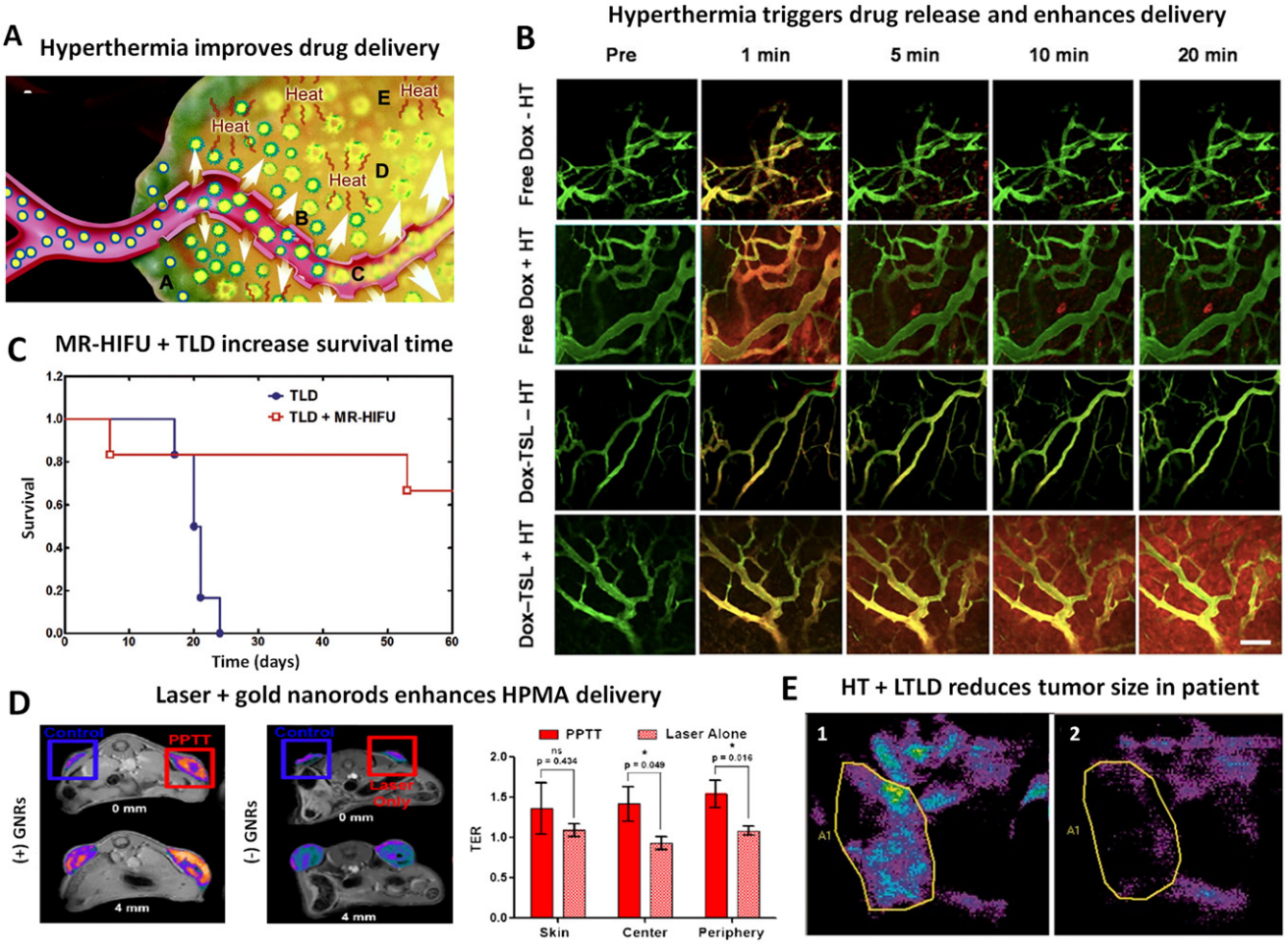

Fig. 6. Hyperthermia. A: Schematic representation of the effects of hyperthermia on drug delivery showing triggered drug release from nanoparticles, exhibiting better distribution and tumor cell killing. B: Intravital microscopy images exemplifying the kinetics of doxorubicin delivery and release from temperature-sensitive liposomes (TSL) upon exposure to mild hyperthermia. GFP-expressing blood vessels are shown in green, doxorubicin is depicted in red. C: Survival of rabbits bearing Vx2 tumors treated with temperature-sensitive liposomal doxorubicin (TLD) versus TLD plus hyperthermia. Hyperthermia was applied using magnetic resonance-guided high-intensity focused ultrasound (MR-HIFU). D: Axial MR images showing enhanced tumor accumulation and improved intratumoral distribution of HPMA copolymer-based drug delivery systems upon hyperthermic pretreatment of tumor using PEGylated gold nanorods (GNRs) and laser light. E: Prior to treatment with low temperature-sensitive liposomal doxorubicin (LTLD), a fairly large tumor mass could be identified in a patient suffering from recurrent breast carcinoma at the chest wall (1). After 4 cycles of LTLD plus hyperthermia, clear evidence was obtained for tumor regression (2). This particular patient went on to achieve a complete local response. Images are reproduced with permission from ref. [58, 62–65].

over time led to an increase in the tumor accumulation of 5-FU, as well as in improved antitumor efficacy (Fig. 5G).

Analogously, Doleschel and colleagues recently reported that also recombinant human erythropoietin (Epo), which has been extensively used for the treatment of chemotherapy-induced anemia, promotes vascular density and enhances perfusion [48]. The results were obtained in two different NSCLC xenograft models (i.e. H838 and A549, respectively). As shown in the functional ultrasound images in Fig. 5H, Epo treatment increased vessel density, perfusion and the relative blood volume in H838 tumors. Histological analysis of Hypoxia-inducible factor-1 (HIF-1) alpha expression was in line with these findings. Epo-mediated vascular promotion consequently enhanced the delivery of carboplatin to tumors (as assessed using inductively coupled plasma mass spectrometry (ICP-MS)), and this resulted in improved antitumor efficacy (Fig. 5I).

Together, the above studies provide initial evidence for the potential of vascular promotion as a novel concept for improving tumor-targeted drug delivery and enhancing antitumor efficacy.

3. Physical treatment

3.1. Hyperthermia

Hyperthermia is an anticancer treatment modality based on the local heating of tumors to temperatures up until ~70 °C, and can be administered in the form of microwaves, radiofrequency and ultrasound (US) [50–52]. Applying mild hyperthermia, in the range of 39–42 °C, promotes perfusion, dilates blood vessels and enhances oxygenation, thereby sensitizing tumors to chemo- and radiotherapy [53,54] (Fig. 6A).

Dewhirst and colleagues investigated the size-dependent liposome accumulation upon hyperthermic treatment using a temperature-controlled window chamber model [55]. Mice bearing ovarian cancer xenografts received i.v. administrations of albumin (~7 nm), as well as 100, 200 and 400 nm-sized liposomes followed by local tumor hyperthermia at 42 °C. The extravasation of albumin remained constant throughout the experiment and was not significantly affected by hyperthermia. Under normothermic conditions (i.e. 34 °C), the accumulation of 100 nm liposomes was significantly lower than that of albumin. The other two liposome formulations (200 and 400 nm) did not extravasate at all. At 42 °C, a significant increase in liposome extravasation was observed, for all liposomes sizes. The 100 nm liposomes showed the highest accumulation upon heating to 42 °C. In a follow-up study, the effects of (1) the applied temperature range, (2) drug administration before vs. during hyperthermia, and (3) consecutive hyperthermia cycles on the tumor accumulation of 100 nm liposomes were studied in an ovarian cancer mouse model [56]. In line with the abovementioned study, liposome extravasation was not pronounced under normothermic conditions (34–39 °C). However, a strong increase in extravasation was recorded upon heating to 40–42 °C. At 42 °C, maximum permeability was reached, and further heating resulted in vascular shutdown. With regard to timing, liposomes accumulation remained to be enhanced up until 6 h after hyperthermia. No further accumulation was observed at later time points, confirming the assumption that the effect of hyperthermia is transient. Interestingly, when hyperthermia was repeated, 8 h after the first heating cycle, no further increase in liposome accumulation was observed, pointing towards acquired thermotolerance by previously pre-heated tumor blood vessels.

Temperature sensitive liposomes (TSL) have evolved as an ideal complimentary platform for co-administration with hyperthermia, enabling triggered drug release locally at the heated tumor site. Several studies have reported on the potential of TSL, showing improved drug delivery and enhanced intratumoral distribution upon combination with mild hyperthermia [57,58]. In this regard, Manzoor and colleagues visualized the intravascular release of doxorubicin from TSL exposed to hyperthermia using intravital microscopy in a skin-fold window chamber tumor model [58]. They showed that temperature-mediated drug delivery enhanced the accumulation and penetration of both free doxorubicin and doxorubicin released from TSL in comparison to normothermia, with the - by far - best results observed for the combination of hyperthermia with TSL (Fig. 6B).

Ponce et al. established MRI-based dose-painting to find the most appropriate protocols for combining TSL with hyperthermia [59]. They quantitatively assessed the temporal and spatial patterns of contrast agent released from lysolipid-based TSL (LTSL) containing doxorubicin and the MRI contrast agent manganese (i.e. Dox/Mn-LTSL) in a rat fibrosarcoma model. Employing contrast-enhanced MRI, they were able to demonstrate that Dox/Mn-LTSL injected during local tumor hyperthermia primarily showed peripheral accumulation, while Dox/Mn-LTSs injected prior to hyperthermia mainly showed enhancement in the central region. Upon administering Dox/Mn-LTSL in a split-dose schedule, uniform distribution could be achieved, with the first half-dose releasing its contents in the central region, and the second half-dose in the peripheral parts. Interestingly, however, in a subsequent therapy study, it was found that Dox/Mn-LTSL administration during hyperthermia generated the strongest treatment response. This was explained on the basis of faster accumulation of LTSL in the peripheral parts and a higher total tumor concentration of released doxorubicin upon employing this regimen (as verified via MRI-based dose-painting).

MRI has played a crucial role in the development of hyperthermia as a therapeutic intervention. It can provide temporal and spatial feedback on the temperature increase in the tumor region (MR thermometry) which, e.g. can help control focused ultrasound (FUS)-mediated heating, and which assists in maintaining optimal temperatures. These notions have led to the development of a hybrid device in which a high intensity-focused ultrasound (HIFU) transducer is integrated in an MRI scanner [60–62]. Employing this device, De Smet, Grüll and colleagues studied the co-release of doxorubicin and the MRI contrast agent Prohance® (i.e. Gd(HPDO3A)(H2O)) from TSL in rats bearing subcutaneous 9L gliosarcomas [61]. TSL co-encapsulating doxorubicin and Prohance® efficiently released high amounts of payload in the tumor region upon mild heating by MR-guided HIFU. MRI provided temperature feedback and enabled real-time monitoring of doxorubicin release by correlating it to simultaneously released Prohance®. Quantification by ICP-MS revealed that the amount of doxorubicin released was in good agreement with that of released gadolinium. The combination of MRI and HIFU is of high clinical value, enabling the visualization and quantification of drug release in real-time, while at the same time allowing for fine-tuning of the employed treatment protocols. Using a similar setup, Staruch and colleagues were able to control the therapeutic effect of doxorubicin-loaded TSL (TLD) in rabbits bearing Vx2 tumors [62]. All rabbits treated with TLD alone, reached the tumor size end point within 24 days of treatment (maximum size > 6 cm), whereas rabbits treated with TLD in combination with mild hyperthermia survived up until 60 days, with only one of them reaching the tumor size end point (Fig. 6C).

As an alternative means to generate heat, Ghandehari and colleagues exploited the surface plasmon resonance effect of gold nanorods (GNRs) to induce hyperthermia and mediate vessel dilation at tumor sites, thereby facilitating the delivery of HPMA (i.e. *N*-(2-hydroxypropyl) methacrylamide) copolymer-based DDS [63]. Mice bearing subcutaneous prostate tumor xenografts (DU-145) on both flanks were treated with GNRs 48 h prior to the administration of Gd-labeled HPMA copolymers and laser irradiation. Only the right flank was irradiated in mice treated with GNRs and the left flank was kept as internal control. GNRs accumulating in the tumor region exhibited rapid heating upon irradiation and the temperature was maintained at 43 °C. MRI revealed that Gd-HPMA copolymers accumulated in much high amounts and were distributed more homogenously in tumor treated with GNRs and laser light compared to control tumor (treated with laser light or GNRs alone; Fig. 6D).

The clinical performance of mild hyperthermia in combination with TSL has been largely in line with preclinical findings. In one of the first

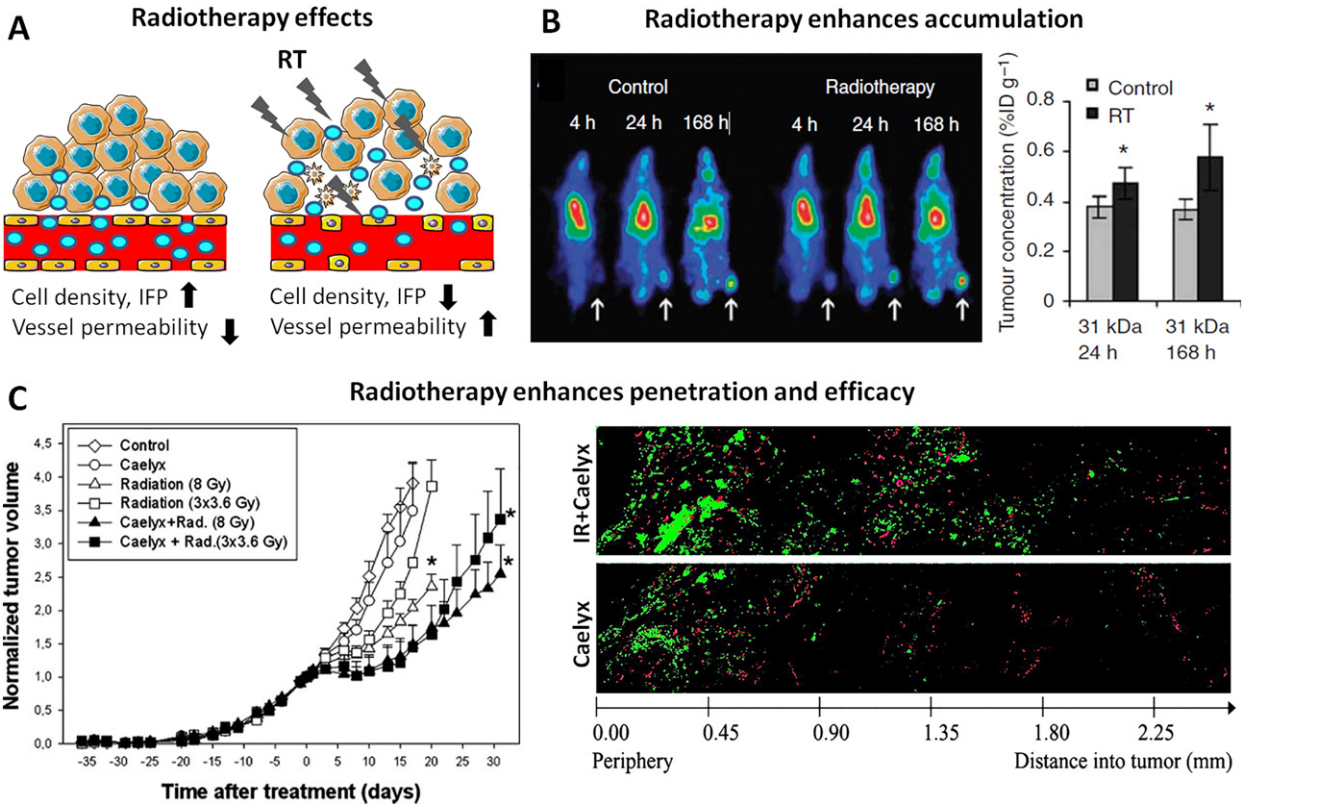

Fig. 7. Radiotherapy. A: Schematic representation illustrating the effects of radiotherapy on drug delivery to the tumor. B: Scintigraphic images showing improved accumulation of ^{131}iodine-labeled HPMA copolymer-based drug delivery systems in Dunning AT1 rat prostate carcinoma tumors upon local radiotherapy treatment at a dose of 20 Gy. C: Tumor growth curves exemplifying significantly enhanced therapeutic effect upon combining PEGylated liposomal doxorubicin (Caelyx) with radiotherapy. The confocal microscopy images on the right show enhanced penetration and distribution of Caelyx (in green) in orthotopic osteosarcoma upon pretreatment with ionizing radiation (IR). Images are reproduced with permission from ref. [67, 68].

key studies, 29 patients with chest wall recurrence of advanced breast cancer were treated with six cycles of low temperature liposomal doxorubicin (LTLD) immediately followed by the application of mild hyperthermia [64]. The combination of LTLD and mild hyperthermia showed an impressive response rate of 48%, with five patients presenting with a complete local response, and with nine patients with a partial response. In this context, Fig. 6F shows the initial antitumor response in a patient who eventually went on to achieve a complete response.

In the phase III HEAT study, performed in patients suffering from hepatocellular carcinoma, LTLD failed to demonstrate benefit as compared to standard radiofrequency ablation (RFA) -based hyperthermia treatment. The reasons for this failure are multifactorial and controversially discussed. Subgroup analyses pointed towards enhanced therapeutic responses for certain patient populations, but the study was not pooled to statistically evaluate such outcomes. The currently ongoing phase III OPTIMA trial is planned more rigorously and monitored more stringently, and it aims to confirm the hypothesis that the combination of RFA with LTLD is able to increase HCC patient survival compared to RFA alone [65].

Summarizing the above efforts and advances, it is obvious that hyperthermia holds significant potential for enhancing the efficacy and the clinical performance of nanomedicine formulations, in particular in case of locally confined tumors.

3.2. Radiotherapy

Radiotherapy is routinely used in approximately half of all solid tumor patients. Besides inducing direct antitumor effects, radiotherapy can also be employed to enhance the tumor accumulation and penetration of drugs and DDS [66–68]. It increases tumor blood vessel permeability via inducing endothelial cell apoptosis and enhancing the expression of vasoactive mediators (e.g. VEGF), and it promotes the penetration of drugs and DDS by lowering the cellular density and the IFP in tumors (Fig. 7A).

As in the case of hyperthermia, the effect of radiotherapy-induced vessel permeability is variable, and depends on radiotherapy dose, on nanocarrier size, on tumor type, and on tumor vascular status prior to treatment [66]. Imaging techniques likes MRI, computed tomography (CT), US, positron emission tomography (PET) and single-photon emission computed tomography (SPECT) have been extensively used to get the insights on the effects of radiotherapy on the tumor vasculature. Schwickert and colleagues employed Gd-labeled albumin and MRI to assess the impact of radiotherapy on vascular permeability in Fischer rats implanted with R3230 mammary adenocarcinomas [66]. 24 h post irradiation, a 15 Gy dose showed a much stronger enhancement of albumin accumulation than a 5 Gy dose. The fractional leak per hour recorded at 24 h after radiotherapy was 0.52 ± 0.08 and 0.87 ± 0.12 for 5 and 15 Gy, respectively, and this was found to be significantly higher than for the untreated control group (0.38 ± 0.05).

Several other studies have exemplified the ability of radiotherapy to enhance tumor-targeted drug delivery. In one of these reports, the positive effect of radiotherapy on the accumulation of HPMA copolymer-based DDS was studied [67]. Rats bearing subcutaneous Dunning AT1 prostate cancer were pretreated with 20 Gy dose of radiotherapy, followed by i.v. administration of ^{131}iodine-labeled HPMA copolymers. Scintigraphic imaging and quantification at 24 h and 168 h provided evidence for enhanced accumulation of the polymers, up to 27% and 57%, respectively (Fig. 7B). In a subsequent therapy study, HPMA copolymer-bound doxorubicin and gemcitabine significantly inhibited tumor

growth when combined with fractionated radiotherapy, while radiotherapy and chemotherapy alone were much less effective.

Similar efforts were invested in assessing the impact of radiotherapy on the penetration, intratumoral distribution and therapeutic efficacy of PEGylated liposomal doxorubicin (Caelyx/Doxil) [68]. A therapy study revealed that combining radiotherapy with liposomal doxorubicin significantly delayed tumor growth in mice bearing osteosarcoma xenografts, whereas liposomal doxorubicin alone had no effect. Histological assessment of tumor tissue specimens showed that radiotherapy led to significantly enhanced liposome accumulation in peripheral and central regions, and improved liposome penetration deep into the tumor interstitium (Fig. 7C).

In line with the above preclinical studies, promising findings have been obtained in patients upon combining the liposomal doxorubicin with radiotherapy [69]. In a first of its kind study performed by Koukourakis and colleagues, seven patients with locally advanced sarcomas were treated with radiotherapy and concomitant administration of radiolabeled PEGylated liposomal doxorubicin [69]. Four out of seven patients achieved a complete response and one showed partial response, resulting in an overall response rate of >70%. No severe toxicities were observed during follow-up. Vice versa, quite severe toxicities have been reported for the combination of radiotherapy with standard chemotherapeutic drugs [70–72], underlining the potential added value of combining radiotherapy with nanomedicine-based drug delivery systems.

Ionizing radiation has also been employed to facilitate the transport of drugs across the BBB [73,74]. In a pilot clinical study, the effect of radiotherapy on the integrity of the BBB was evaluated in 14 patients with intracranial tumors with a largely intact BBB by employing the brain imaging agent ^{99m}Tc-glucoheptonate (^{99m}Tc-GH) [73]. This study revealed that a cumulative radiotherapy dose in the range of 30–40 Gy efficiently disrupted the BBB in tumors. Based on this notion, the authors

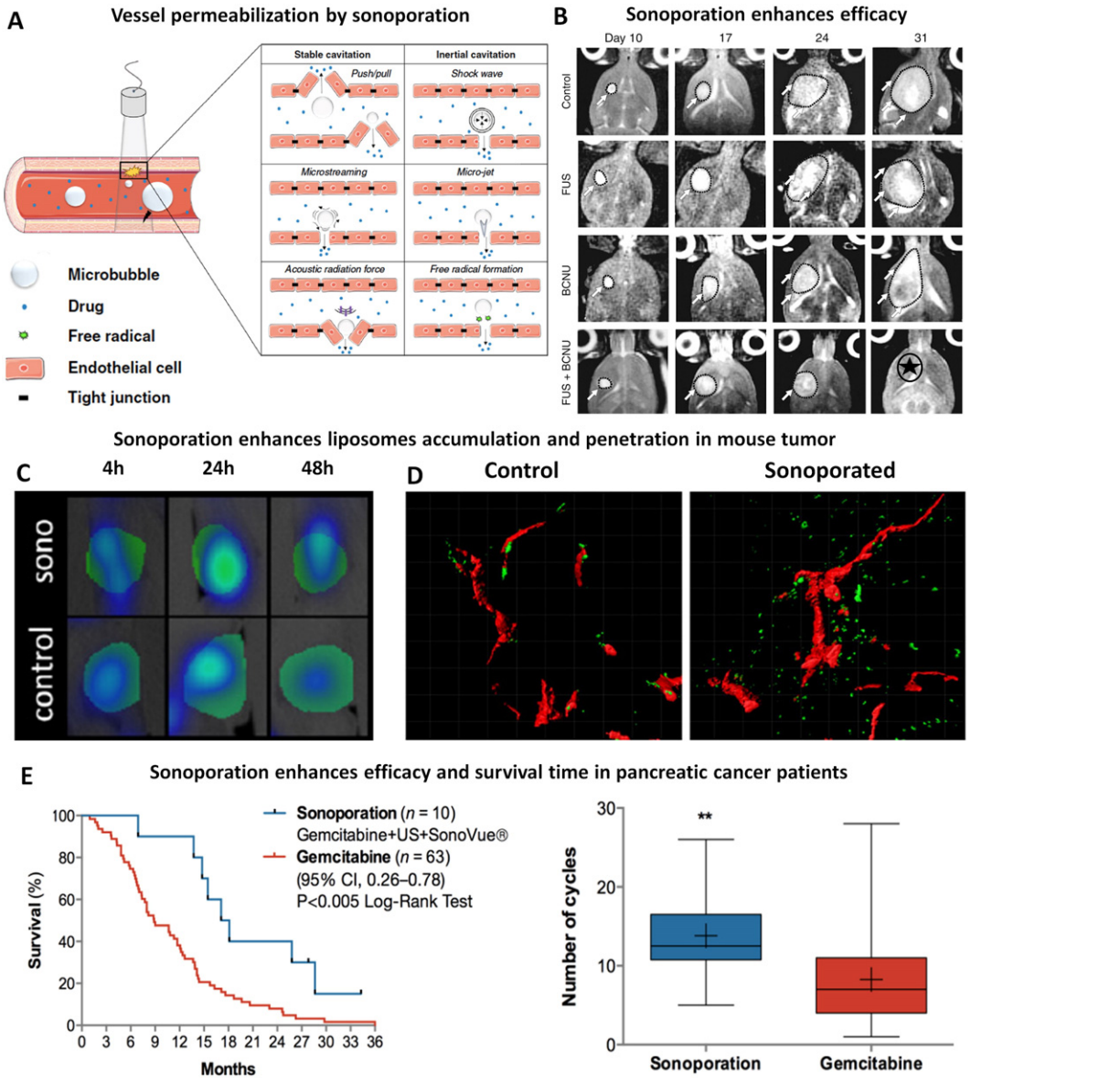

Fig. 8. Sonoporation. A: Mechanisms by which sonoporation improves vessel permeability, based on stable and inertial microbubble (MB) cavitation. B: T2-weighted MR images showing enhancement of glioma treatment in rats upon combining BCNU-based chemotherapy with sonoporation (i.e. FUS + MB). * Indicates complete tumor shrinkage at day 31. C: Hybrid CT-FMT imaging exemplifying enhanced accumulation of fluorophore-labeled PEGylated liposomes in tumors treated with sonoporation. D: Multi-photon microscopy images demonstrating enhanced penetration of fluorophore-labeled PEGylated liposomes (green) out of rhodamine-lectin-stained blood vessels (red) upon sonoporation. E: Survival curves of pancreatic cancer patients treated with gemcitabine with and without sonoporation co-treatment. The number of treatment cycles that could be administered to these patients is shown on the right. Images reproduced with permission from ref. [78, 83, 87, 88].

suggested that in postoperative brain tumor treatment, radiotherapy should be followed by chemotherapy to obtain improved therapeutic effects. In a follow-up study by the same group of scientists, 28 patients suffering from glioblastoma were treated with 20–40 Gy of radiotherapy followed by treatment with alkylating chemotherapeutic drug chloroethyl-cyclohexyl-nitrosourea (CCNU) [74]. The outcome was compared to a historical cohort of 28 patients treated with radiotherapy alone. In the radio-chemotherapy group, responses were substantially enhanced, as exemplified by 1-, 3- and 5-year survival rates of 57, 23 and 15%, as compared to 18, 7 and 4% for radiotherapy alone.

Together, the above studies convincingly demonstrate that radiotherapy may be able to improve several aspects of tumor-targeted drug delivery, and they indicate that rationally designed (nano-) chemo-radiotherapy regimens may hold significant clinical potential.

3.3. Sonoporation

Sonoporation refers to the permeabilization of cell membranes induced by the rapid expansion and compression (and/or collapse) of microbubbles (MB) upon exposure to US [75]. Historically, sonoporation has been mainly used to achieve intracellular delivery of large and/or charged molecules, like DNA, which are not readily taken up by cells [75–77]. Given the fact that systemically administrated MB – because of their size – are generally confined to the vascular compartment, it has to be realized that in vivo, oscillating or imploding MB primarily affect the endothelial lining, promoting the extravasation of drug and DDS into the interstitial space (Fig. 8A) [78].

Before assessing the impact of sonoporation on drug delivery to tumors, the effect of combining US with MB was studied in the brain. In 2001, Hynynen and colleagues for the first time evaluated BBB opening in rabbits, by combining focused US (FUS) and MB and by employing MRI for the real-time monitoring of model drug delivery to the brain [79]. In comparison to FUS alone, the administration of MB enabled opening of the BBB at much lower US energies, and it caused no permanent damage to the brain. Several years later, the same group of scientists successfully demonstrated delivery of large therapeutic compounds, i.e. Herceptin, across the BBB mediated upon prior treatment with FUS and MB [80]. BBB opening was monitored by assessing the accumulation of the MRI contrast agent Magnevist in the brain, and this was found to be in good agreement with Herceptin delivery. Using similar experimental settings, the authors also demonstrated delivery of liposomal doxorubicin across the BBB [81].

Extending the above efforts towards MRI-guided sonoporation as a safe and reliable strategy for shuttling drugs and DDS across the BBB, Koczera and colleagues developed poly (butyl cyanoacrylate)-based MB carrying ultra-small superparamagnetic iron oxide (USPIO) nanoparticles within their shell [82]. The rationale behind developing USPIO-MB system was to at the same time mediate and monitor BBB opening. This was achieved by employing transcranial US to destroy USPIO-MB in CD-1 nude mice, and by assessing the extravasation of released USPIO (and USPIO retained in PBCA MB shell fragments) in brain tissue by T2*-weighted MRI. 2D and 3D microscopy was employed to determine the extravasation of co-administered fluorescein isothiocyanate (FITC)-dextran, which served as a macromolecular model drug. Significant extravasation and accumulation of FITC-dextran in brain tissue was observed upon sonoporation, and this was found to be in line with the MRI measurements.

Liu et al. assessed the feasibility and safety profile of FUS- plus MB-mediated anticancer drug delivery in rats bearing orthotopic C6 gliomas [83]. As exemplified by Fig. 8B, they showed that sonoporation was able to significantly enhance the intratumoral distribution of 1,3-bis(2-chloroethyl)-1-nitrosourea (BCNU), leading to improved antitumor responses and to a prolongation of the median survival time. Histological analysis of treated brain tissue showed that sonoporation may induce intracerebral hemorrhages, but the incidence of this was found to be low. By combining sonoporation with (MR) imaging, the frequency and intensity of such adverse events can likely be controlled.

To move towards the use of sonoporation in patients, McDannold and colleagues employed a clinically relevant transcranial MR-guided FUS setup to open up the BBB in non-human primates [84]. They demonstrated reliable and repeated opening of the BBB in rhesus macaques, and the settings employed did not result in obvious tissue damage or abnormal brain function. Following up on these efforts, in November 2015, sonoporation for the first time was used to permeate the BBB in patients [85]. More specifically, FUS and MB were used in glioblastoma patients to improve the accumulation and efficacy of doxorubicin. This study is performed by Hynynen and colleagues at the Sunnybrook Health Sciences Center in Toronto, and the initial outcomes of this study are eagerly awaited. Another clinical trial has been initiated by Carpentier, Idbaih and colleagues in which implantable US device (SonoCloud) and phospholipid MB are employed to deliver carboplatin across the BBB in patients suffering from recurrent glioblastoma [86]. The preliminary data shows successful transient opening of the BBB at acoustic pressures up to 1.1 MPa, which was well tolerated by the patients. However, it was impossible to sonicate the whole tumor, as the sonication field width of the transducer was smaller than the width of the tumor. Nonetheless, the results are encouraging and further studies looking at the overall efficacy of this approach are warranted.

In recent years, sonoporation has also been increasingly employed to treat pathologies outside of the brain. Theek and colleagues, for instance, assessed the impact of sonoporation on the accumulation of PEGylated liposomes in two different tumor models characterized by low baseline levels of EPR, i.e. highly cellular A431 epidermoid xenografts and highly stromal BxPC-3 pancreatic carcinoma xenografts [87]. MB and double-fluorophore-labeled liposomes were co-injected intravenously, and MB were then locally destroyed in the tumor region by US. Using in vivo computed tomography-fluorescence molecular tomography (CT-FMT) imaging and ex vivo multi-photon microscopy, it was shown that sonoporation is able to enhance both the accumulation and the penetration of liposomes in both the tumor models (Fig. 8C–D).

Extending these findings to the clinic, Dimcevski and colleagues recently reported a pioneering phase 1 clinical trial in which ten patients with pancreatic cancer were treated with gemcitabine in combination with US and MB [88]. The outcome of this study was encouraging, showing a decrease in tumor volume in five patients and a delay in tumor growth progression in the other five patients. As compared to a historical cohort, an impressive increase in median survival was achieved, from 6.7 months to 17.6 months, respectively (Fig. 8E). In addition, the treatment was found to be relatively well tolerated by all the patients. Obvious downsides of this study are the low number of patients that were included and the fact that the comparison relied on a historical cohort, making it difficult to draw definite conclusions. Nevertheless, these proof-of-principle findings suggest that sonoporation may be a very useful vessel modulation treatment to try to improve the treatment of malignancies which are notoriously difficult to treat, such as pancreatic cancer.

3.4. Phototherapy

Photodynamic therapy (PDT) is an increasingly popular anticancer treatment which is based on local or systemic administration of photosensitizers followed by local irradiation with laser light of a specific wavelength. Upon exposure to light, photosensitizers absorb photons, raising their energy levels from the ground singlet state to the excited state. Subsequent relaxation back to the ground state leads to the generation of singlet oxygen and other reactive oxygen species, which cause cell damage and induce apoptosis [89,90].

PDT is also known to elicit toxic effects on endothelial cells, leading to enhanced vascular leakiness and/or vascular shutdown [91–95]. Sporn and Foster studied the effect of PDT on cultured human endothelial cells and reported that it induces cytoplasmic microtubule depolymerization, which results in cell contraction and rounding [94]. This

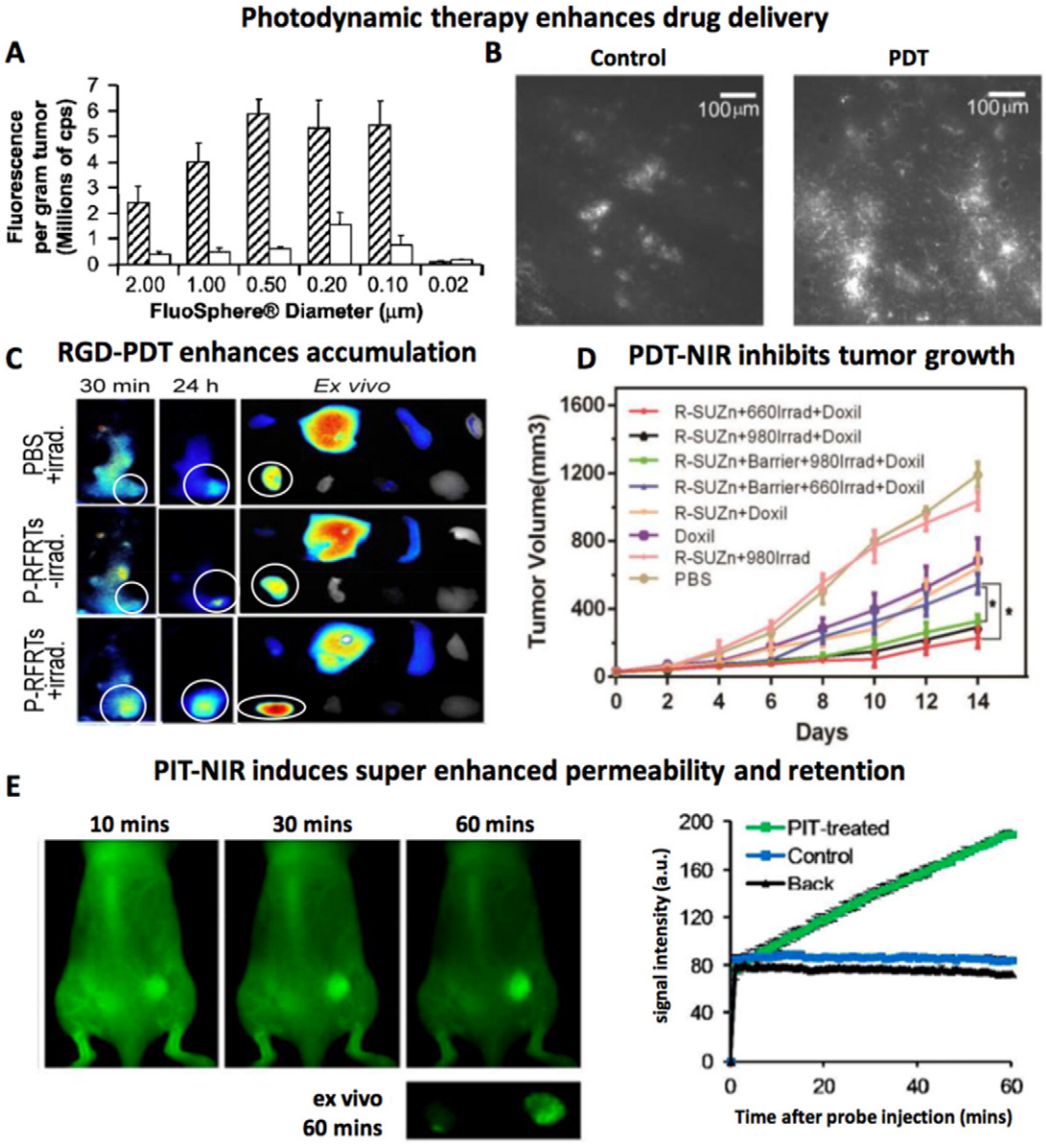

Fig. 9. Phototherapy. A: Pretreatment with photodynamic therapy (PDT) increases the tumor accumulation of FluoSpheres with sizes of 100 to 2000 nm. B: Increase in PEGylated liposomal doxorubicin accumulation upon PDT pretreatment. C: In vivo and ex vivo fluorescence reflectance imaging demonstrating improved tumor accumulation of fluorophore-labeled human serum albumin upon treatment with photosensitizer loaded RGD-ferritin plus laser irradiation (P-RFRTs + irrad). Tumors are encircled. D: Phototherapy based on R-SUZn a novel PDT agent comprising of RGD conjugated photosensitizer with photon upconversion nanoparticles combined with near-infrared laser light (NIR: 980 nm) and visible light (660 nm) improves the antitumor efficacy of PEGylated liposomal doxorubicin (Doxil). In the presence of a 1 cm-thick tissue barrier, only the combination of R-SUZn plus NIR laser irradiation improved tumor growth inhibition. E: Optical imaging illustrating "super enhanced permeability and retention (SUPR)" of 50 nm sized quantum dots in tumors treated with photoimmunotherapy (PIT). Images reproduced with permission from ref. [95–97, 100].

notion promotes vascular leakiness by increasing the gaps between individual endothelial cells. In line with this, Fingar and colleagues performed intravital microscopy on rat muscle tissue to study the impact of PDT on vascular constriction, permeability and leukocyte adhesion [91]. When combined with local light administration, a dose of 25 mg/kg photofrin induced arteriole constriction followed by venule constriction, as well as an increase in vessel permeability to albumin. An increase in leukocyte adhesion to venule endothelium was also observed after PDT treatment, which could further promote vessel permeability via multiple signaling pathways.

Extending these findings, Snyder et al. reported the use of PDT for facilitating the delivery of model macromolecular drug carriers [95]. In a murine colon cancer tumor model, they employed low fluences and fluence rates (ranging from 13 to 128 J/cm^2 and 3.5 to 112 mW/cm^2) to induce vessel permeabilization without causing vascular shutdown. To study the effect of PDT on vascular permeability, FluoSpheres having sizes ranging from 20 to 2000 nm were intravenously administered immediately after PDT (using 2-[1-hexyloxyethyl]-2-devinyl pyropheophorbide-a (HPPH) as the photosensitizer). High accumulation of FluoSpheres was recorded in fluence and fluence rate ranges of 48–88 J/cm^2 and 14–28 mW/cm^2, respectively. Maximal accumulation was observed for particles in the size range of 100–500 nm (Fig. 9A). In line with this, also the accumulation of 100 nm-sized PEGylated liposomal doxorubicin was found to be increased upon PDT treatment (Fig. 9B).

To promote the selectivity and performance of photosensitizers, Zhen et al. developed RGD-modified and $ZnF_{16}Pc$-loaded ferritin (P-RFRTs), to target overexpressed $\alpha_v\beta_3$ integrins on the tumor endothelium [96]. They evaluated the effect of this targeted photosensitizer formulation and PDT treatment on the accumulation of human serum albumin (HSA), quantum dots and iron oxide nanoparticles in four different tumor models. Fig. 9C exemplifies the enhanced accumulation of

fluorophore-labeled HSA in 4 T1 tumors treated with P-RFRT-based PDT. One day after HSA injection, a 2.4-fold increase in HSA uptake was observed in illuminated tumors as compared to non-treated control tumors.

One of the downsides of using PDT to enhance vascular permeability and drug delivery is that its effects are compromised in deeper seated tumors. This is because of the limited penetration depth of light, which is even worsened by the fact that light in the visible range has to be used to excite photosensitizers. Gao and colleagues set out to address this problem, at least to some extent, by developing a PDT platform which allows for the use of near-infrared light (NIR), enabling better tissue penetration [97]. They designed c(RGDyK)-SOC-UCNP-ZnPc (R-SUZn), a novel PDT agent which consists of upconversion nanoparticles (UCNPs), amphiphilic chitosan, zinc phthalocyanine (ZnPc) and an $\alpha_v\beta_3$ targeting ligand c(RGDyK). The employed UCNPs are lanthanide-doped nanocrystals, which emit high-energy photons when excited by NIR light, resulting in the activation of the co-incorporated ZnPC photosensitizer. The usefulness of this system was demonstrated by irradiation of R-SUZn with low fluence NIR light followed by i.v. administration of Doxil in mice bearing subcutaneous PC-3 prostate adenocarcinoma tumors. To mimic deep tissue penetration of the employed laser light, the subcutaneous tumors were overlaid with a 1 cm thick piece of pork tissue. For head-to-head comparison with conventional illumination, tumors treated with R-SUZn were also irradiated with standard 660 nm laser light in the presence of the 1 cm pork tissue barrier. As hypothesized, R-SUZn irradiation with 660 nm light did not enhance the efficacy of Doxil as compared to treatment with Doxil alone, indicating that light in this range is incapable of penetrating thick tissue. On the other hand, as exemplified in Fig. 9D, when R-SUZn-treated tumors were irradiated with 980 nm NIR laser light, significantly enhanced tumor shrinkage was achieved upon combination with Doxil.

Photoimmunotherapy (PIT), which is based on the use of antibody-photosensitizer conjugates, is another interesting PDT regimen [98,99]. By causing cytotoxicity in (cancer) cells in perivascular regions, it may help to lower the IFP and decompress the tumor blood vessels. These effects contribute to improved perfusion, as well as to enhanced extravasation and penetration of drugs and DDS. Kobayashi and colleagues have achieved impressive results with PIT. They employed the FDA-approved EGFR-binding antibody panitumumab for targeted delivery of the photosensitizer Pan-IR700 to EGFR-overexpressing A431 tumor cells [100]. The effect of PIT on EPR-mediated tumor accumulation was evaluated by using 50 nm-sized PEGylated quantum dots (Qdot800) and 200 nm-sized super-paramagnetic iron oxide nanoparticles (SPION) as model DDS. A strong enhancement in Qdot800 accumulation was observed in PIT-treated tumors: from 10 to 60 min after Qdot800 administration, the levels localizing to tumors were >25 times higher than in control tumors (Fig. 9E). Enhanced accumulation was also observed for the larger iron oxide nanoparticles. Because of these very strong increases in accumulation induced by PIT, the authors referred to this effect as "super enhanced permeability and retention" (SUPR). In a follow-up report, the authors studied the effect of NIR light dosing at different time intervals on the tumor penetration of circulating photosensitizers in MDA-MB468luc tumors and A431luc tumor models [101]. The results indicated that multiple NIR light exposures at intervals of 3 to 6 h after the first illumination enhance the tumor penetration of photosensitizers compared to repeated illumination at 24 h after i.v. injection (standard protocol). This new regimen compared to the standard protocol allows single dose photosensitizer therapy with multiple light exposure at the same day and hence is more convenient for patients.

Together, the above studies demonstrate the potential of using phototherapy to enhance vessel permeability and the accumulation of drugs and drug delivery systems.

4. Summary and future perspectives

Many nanomedicine formulations have been evaluated over the years, in particular for the treatment of cancer. The tumor accumulation and therapeutic efficacy of nanomedicines strongly depends on the EPR effect, which can be highly heterogeneous. Several pharmacological (permeabilization, normalization, disruption and promotion) and physical (hyperthermia, radiotherapy, sonoporation and phototherapy) vessel modulation strategies have been evaluated for improving EPR-mediated tumor targeting. They have been shown to be able to enhance the tumor accumulation of drugs and drug delivery systems by 2-3-fold and in exceptional cases (e.g. upon PIT-induced super EPR) even by more than a 20-fold, and they have contributed to improved therapeutic responses in a variety of tumor models.

The potential added value of the above strategies strongly depends on their availability and their clinical status. In this context, pharmacological modulation with clinically approved and extensively used vasomodulators, such as losartan or bevacizumab, may be an attractive method for trying to improve tumor accumulation and intratumoral distribution. One of the key assets of pharmacological modulation is that these agents - upon oral or intravenous administration - are able to elicit effects all over the body, and consequently are useful for treating patients with metastases. It has to be kept in mind, however, that the response of individual patients to such pharmacological modulators can be quite variable.

Physical vessel modulation strategies can be applied in a temporally and spatially better controlled manner, and as compared to pharmacological interventions, their effects are expected to be more homogenous and more reproducible. Moreover, multiple physical modalities are already well established in the clinic, and therefore relatively easy to put into practice. The downside of all physical strategies, however, is that they are locally confined, and thus are not very useful for the treatment of metastatic disease.

Future research should focus on applying the right vessel modulation strategy (and the right (nano-) combination treatment) in the right patient. Consequently, methods are needed to identify which patients are the right ones. In this context, in particular in the case of patients suffering from metastatic disease, the use of noninvasive imaging is considered to be crucial, not only to at some point assess nanomedicine accumulation, but particularly also to stratify patients on the basis of vascular characteristics, prior to vessel modulation therapy [102–104]. This reasoning is exemplified in a simplified form in Fig. 10, in which patients with solid tumors and metastases are stratified on the basis of vascular characteristics, so that they can be better assigned to the right therapy. The first step in this process would be the anatomical identification of primary tumors and metastases. This should ideally be done using whole-body hot-spot imaging techniques, such as PET or SPECT. The second step would involve functional imaging of the properties of the vasculature in tumors and metastases. This can e.g. be done using dynamic contrast-enhanced MRI, providing quantitative information on blood vessel density, blood vessel perfusion and vascular permeability.

Based on the insights obtained, suitable vessel modulation strategies can then be selected for individual patients. For instance, patients having tumors characterized by high vessel density and low permeability can then be assigned to pharmacological strategies that potentiate leakiness, such as permeabilization and disruption, as well as to permeabilization-promoting physical treatments, such as sonoporation. Patients with tumors characterized by low vessel density and low permeability generally present with very poor accumulation and intratumoral distribution of drugs and drug delivery systems. In such cases, patients should be assigned to vessel promotion, which enhances vascular density and which may also increase leakiness. Combinations with physical strategies, such as hyperthermia and sonoporation, can help to decompress vessels and further enhance vascular permeability, together resulting in improved accumulation, distribution and efficacy of drugs and drug delivery systems.

There is still a long way to go, however, before such 'personalized' vessel modulation therapies can be implemented in the clinic. Multiple arguments can be envisaged on why this is the case. Among them is the fact that the abovementioned imaging protocols to assess the vascular density

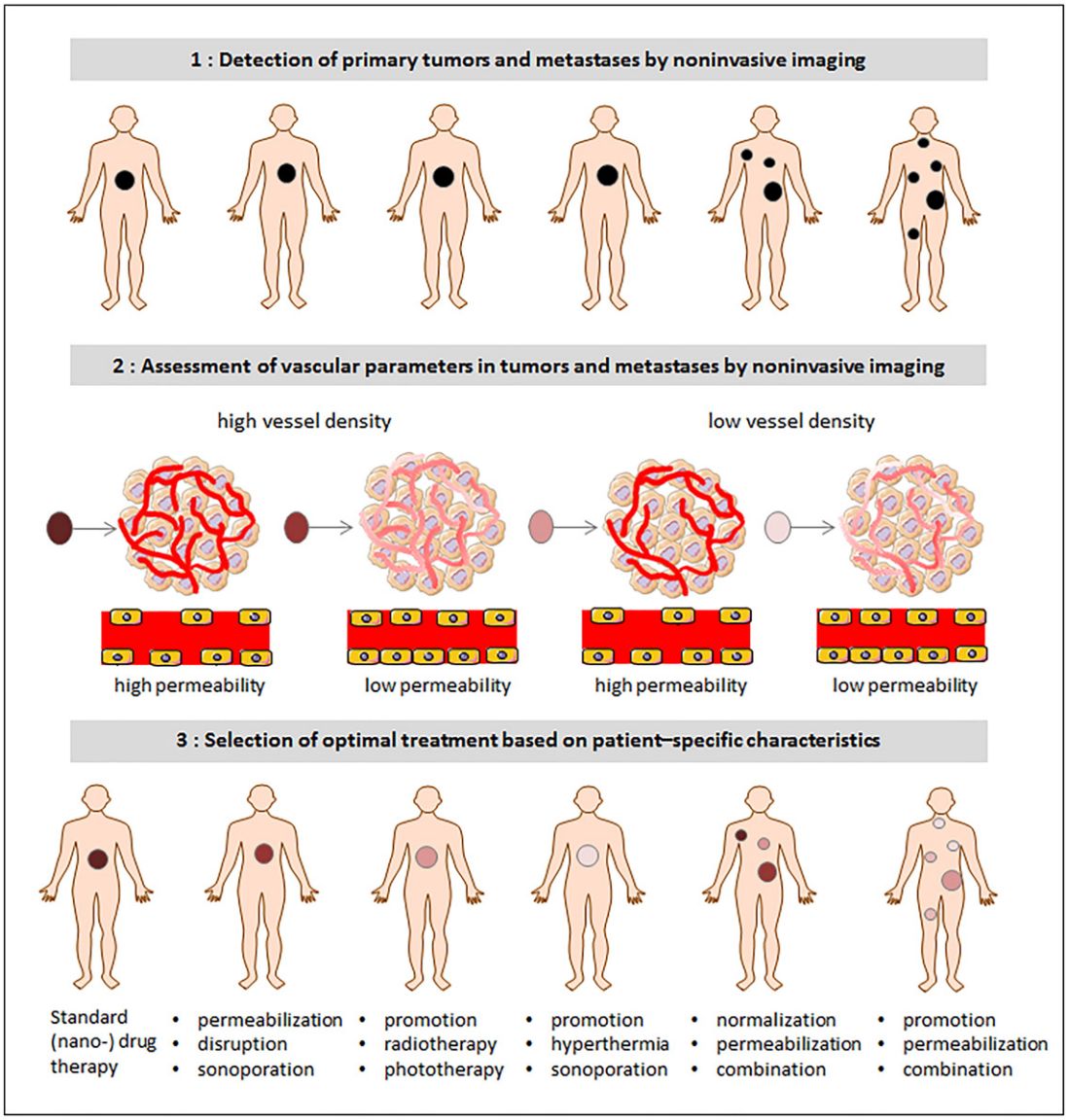

Fig. 10. Rationale for personalized combinations of vessel modulation therapy with tumor-targeted (nano-) drug therapy. Based on noninvasive imaging information on the location and number of primary tumors and metastases (1st step), as well as on imaging-based assessment of vessel density and permeability (2nd step), patients can be preselected for optimal vessel modulation therapy. Upon identifying patient-specific characteristics of the tumor vasculature, individuals can either be assigned to physical treatment (especially in case of locally confined tumors), or to systemic pharmacological interventions (in case of metastatic disease). Upon vessel priming, these patients can likely be treated much more efficiently with tumor-targeted nanomedicine formulations.

and permeability are not routinely performed in patients. Furthermore, evidence-based medicine requires systematic comparisons, e.g. of patients with vs. patients without vascular modulation treatment, to demonstrate that a given combination therapy really works. Such studies are unfortunately hardly ever performed, because in many of these situations, the financial incentives to combine two existing treatments may not be given. At the same time, novel combination therapies always bear the risk of resulting in unexpected and/or severe side effects, which may be detrimental for drugs and drug developers. It therefore seems likely that the majority of these trials will have to be investigator-initiated, rather than pharma-sponsored. Which means that moving forward and making progress is more difficult, and goes slower, and that funding has to be (mostly) provided by governmental and/or healthcare organizations. This should, however, not withhold us from performing such studies. Several of the investigator-initiated vessel modulation trials mentioned above, e.g. the ones employing isolated-limb perfusion in sarcoma, vascular normalization in glioblastoma and sonoporation in pancreatic cancer, illustrate that we can learn a lot from such studies, and that they might be very valuable for helping us shape the future face of cancer therapy.

Finally, in the future, it will be crucial to go beyond vessel modulation, towards remodeling of the whole microenvironment in tumors and metastases. And to not only focus on the impact of vessel and microenvironment modulation on the accumulation and efficacy of drugs and drug delivery systems, but to also employ these strategies to prime malignant lesions for novel types of treatment, such as immunotherapy. This has recently made many headlines and it might indeed boost the number of cancer cures, but only if the vasculature and the microenvironment allow for proper extravasation and penetration of antibodies and T cells into tumors and metastases. From this perspective - and of course also from a nanomedicine and drug targeting point of view - it is clear that we have to keep on investing in strategies to modulate tumor blood vessels and the microenvironment, and that we should try harder to make them part of clinical practice. This requires dedicated and concerted actions, and interdisciplinary research teams, in which academic scientists and clinicians intensively interact with pharmaceutical companies and regulatory agencies, to together establish better combination treatments for patients suffering from cancer.

Acknowledgements

The authors gratefully acknowledge financial support by the European Union (EU H2020-MSCA-ITN-2014 642 028-NABBA), by the European Research Council (ERC Starting Grant 309495 (NeoNaNo) and ERC Proof-of-Concept Grant 680882 (CONQUEST)), by the German Research Foundation (DFG La2937/1-2 and SFB1066) and by the German Academic Exchange Program (DAAD 57214224).

References

[1] Y. Matsumura, H. Maeda, A new concept for macromolecular therapeutics in cancer chemotherapy: mechanism of tumoritropic accumulation of proteins and the antitumor agent smancs, Cancer Res. 46 (1986) 6387–6392.
[2] K.J. Harrington, S. Mohammadtaghi, P.S. Uster, D. Glass, A.M. Peters, R.G. Vile, J.S.W. Stewart, Effective targeting of solid tumors in patients with locally advanced cancers by radiolabeled pegylated liposomes, Clin. Cancer Res. 7 (2001) 243–254.
[3] M. Koukourakis, S. Koukouraki, A. Giatromanolaki, S. Archimandritis, J. Skarlatos, K. Beroukas, J. Bizakis, G. Retalis, N. Karkavitsas, E. Helidonis, Liposomal doxorubicin and conventionally fractionated radiotherapy in the treatment of locally advanced non–small-cell lung cancer and head and neck cancer, J. Clin. Oncol. 17 (1999) 3512–3521.
[4] P. Carmeliet, R.K. Jain, Angiogenesis in cancer and other diseases, Nature 407 (2000) 249–257.
[5] J. Fang, H. Nakamura, H. Maeda, The EPR effect: unique features of tumor blood vessels for drug delivery, factors involved, and limitations and augmentation of the effect, Adv. Drug Deliv. Rev. 63 (2011) 136–151.
[6] H. Maeda, Vascular permeability in cancer and infection as related to macromolecular drug delivery, with emphasis on the EPR effect for tumor-selective drug targeting, Proc. Jpn. Acad. Ser. B Phys. Biol. Sci. 88 (2012) 53–71.
[7] K.J. Tracey, A. Cerami, Tumor necrosis factor, other cytokines and disease, Annu. Rev. Cell Biol. 9 (1993) 317–343.
[8] M. Krajnik, Z. Zylicz, Understanding pruritus in systemic disease, J. Pain Symptom Manag. 21 (2001) 151–168.
[9] A. Eggermont, H. Schraffordt Koops, D. Liénard, B. Kroon, A.N. van Geel, H.J. Hoekstra, F.J. Lejeune, Isolated limb perfusion with high-dose tumor necrosis factor-alpha in combination with interferon-gamma and melphalan for nonresectable extremity soft tissue sarcomas: a multicenter trial, J. Clin. Oncol. 14 (1996) 2653–2665.
[10] F. Lejeune, D. Lienard, A. Eggermont, H.S. Koops, F. Rosenkaimer, J. Gerain, J. Klaase, B. Kroon, J. Vanderveken, P. Schmitz, Rationale for using TNFα and chemotherapy in regional therapy of melanoma, J. Cell. Biochem. 56 (1994) 52–61.
[11] T. Seki, F. Carroll, S. Illingworth, N. Green, R. Cawood, H. Bachtarzi, V. Šubr, K.D. Fisher, L.W. Seymour, Tumour necrosis factor-alpha increases extravasation of virus particles into tumour tissue by activating the Rho A/Rho kinase pathway, J. Control. Release 156 (2011) 381–389.
[12] J.J. Connell, G. Chatain, B. Cornelissen, K.A. Vallis, A. Hamilton, L. Seymour, D.C. Anthony, N.R. Sibson, Selective permeabilization of the blood–brain barrier at sites of metastasis, J. Natl. Cancer Inst. 21 (2013) 1634–1643.
[13] K.L. Black, D. Yin, J.M. Ong, J. Hu, B.M. Konda, X. Wang, M.K. Ko, J.-A. Bayan, M.R. Sacapano, A. Espinoza, PDE5 inhibitors enhance tumor permeability and efficacy of chemotherapy in a rat brain tumor model, Brain Res. 1230 (2008) 290–302.
[14] W.P. Arnold, C.K. Mittal, S. Katsuki, F. Murad, Nitric oxide activates guanylate cyclase and increases guanosine 3′: 5′-cyclic monophosphate levels in various tissue preparations, Proc. Natl. Acad. Sci. 74 (1977) 3203–3207.
[15] R.M. Palmer, A. Ferrige, S. Moncada, Nitric oxide release accounts for the biological activity of endothelium-derived relaxing factor, Nature 327 (1987) 524–526.
[16] T. Seki, J. Fang, H. Maeda, Enhanced delivery of macromolecular antitumor drugs to tumors by nitroglycerin application, Cancer Sci. 100 (2009) 2426–2430.
[17] K. Hori, M. Suzuki, S. Tanda, S. Saito, M. Shinozaki, Q.H. Zhang, Fluctuations in tumor blood flow under normotension and the effect of angiotensin II-induced hypertension, Jpn. J. Cancer Res. 82 (1991) 1309–1316.
[18] A.K. Iyer, G. Khaled, J. Fang, H. Maeda, Exploiting the enhanced permeability and retention effect for tumor targeting, Drug Discov. Today 11 (2006) 812–818.
[19] R.K. Jain, Normalization of tumor vasculature: an emerging concept in antiangiogenic therapy, Science 307 (2005) 58–62.
[20] R.K. Jain, Normalizing tumor vasculature with anti-angiogenic therapy: a new paradigm for combination therapy, Nat. Med. 7 (2001) 987–989.
[21] S. Goel, A.H.-K. Wong, R.K. Jain, Vascular normalization as a therapeutic strategy for malignant and nonmalignant disease, Cold Spring Harb. Perspect. Med. 2 (2012) a006486.
[22] R.T. Tong, Y. Boucher, S.V. Kozin, F. Winkler, D.J. Hicklin, R.K. Jain, Vascular normalization by vascular endothelial growth factor receptor 2 blockade induces a pressure gradient across the vasculature and improves drug penetration in tumors, Cancer Res. 64 (2004) 3731–3736.
[23] V.P. Chauhan, T. Stylianopoulos, J.D. Martin, Z. Popović, O. Chen, W.S. Kamoun, M.G. Bawendi, D. Fukumura, R.K. Jain, Normalization of tumour blood vessels improves the delivery of nanomedicines in a size-dependent manner, Nat. Nanotechnol. 7 (2012) 383–388.
[24] C.G. Willett, Y. Boucher, E. Di Tomaso, D.G. Duda, L.L. Munn, R.T. Tong, D.C. Chung, D.V. Sahani, S.P. Kalva, S.V. Kozin, Direct evidence that the VEGF-specific antibody bevacizumab has antivascular effects in human rectal cancer, Nat. Med. 10 (2004) 145–147.
[25] T.T. Batchelor, E.R. Gerstner, K.E. Emblem, D.G. Duda, J. Kalpathy-Cramer, M. Snuderl, M. Ancukiewicz, P. Polaskova, M.C. Pinho, D. Jennings, Improved tumor oxygenation and survival in glioblastoma patients who show increased blood perfusion after cediranib and chemoradiation, Proc. Natl. Acad. Sci. 110 (2013) 19059–19064.
[26] R.K. Jain, D.G. Duda, J.W. Clark, J.S. Loeffler, Lessons from phase III clinical trials on anti-VEGF therapy for cancer, Nat. Clin. Pract. Oncol. 3 (2006) 24–40.
[27] S.M. Tolaney, Y. Boucher, D.G. Duda, J.D. Martin, G. Seano, M. Ancukiewicz, W.T. Barry, S. Goel, J. Lahdenrata, S.J. Isakoff, Role of vascular density and normalization in response to neoadjuvant bevacizumab and chemotherapy in breast cancer patients, Proc. Natl. Acad. Sci. 112 (2015) 14325–14330.
[28] J.-S. Park, I.-K. Kim, S. Han, I. Park, C. Kim, J. Bae, S.J. Oh, S. Lee, J.H. Kim, D.-C. Woo, Normalization of tumor vessels by Tie2 activation and Ang2 inhibition enhances drug delivery and produces a favorable tumor microenvironment, Cancer Cell 30 (2016) 953–967.
[29] R.K. Jain, Normalizing tumor microenvironment to treat cancer: bench to bedside to biomarkers, J. Clin. Oncol. 31 (2013) 2205–2218.
[30] E. Brown, T. McKee, A. Pluen, B. Seed, Y. Boucher, R.K. Jain, Dynamic imaging of collagen and its modulation in tumors in vivo using second-harmonic generation, Nat. Med. 9 (2003) 796–800.
[31] V.P. Chauhan, J.D. Martin, H. Liu, D.A. Lacorre, S.R. Jain, S.V. Kozin, T. Stylianopoulos, A.S. Mousa, X. Han, P. Adstamongkonkul, Angiotensin inhibition enhances drug delivery and potentiates chemotherapy by decompressing tumour blood vessels, Nat. Commun. 4 (2013) 2516.
[32] T.E. Peterson, N.D. Kirkpatrick, Y. Huang, C.T. Farrar, K.A. Marijt, J. Kloepper, M. Datta, Z. Amoozgar, G. Seano, K. Jung, Dual inhibition of Ang-2 and VEGF receptors normalizes tumor vasculature and prolongs survival in glioblastoma by altering macrophages, Proc. Natl. Acad. Sci. 113 (2016) 4470–4475.
[33] D. Beauregard, P. Thelwall, D. Chaplin, S. Hill, G. Adams, K. Brindle, Magnetic resonance imaging and spectroscopy of combretastatin A4 prodrug-induced disruption of tumour perfusion and energetic status, Br. J. Cancer 77 (1998) 1761–1767.
[34] D.W. Siemann, The unique characteristics of tumor vasculature and preclinical evidence for its selective disruption by tumor-vascular disrupting agents, Cancer Treat. Rev. 37 (2011) 63–74.
[35] G. Tozer, C. Kanthou, G. Lewis, V. Prise, B. Vojnovic, S. Hill, Tumour vascular disrupting agents: combating treatment resistance, Br. J. Radiol. 81 (2014) S12–S20.
[36] Q. Ng, H. Mandeville, V. Goh, R. Alonzi, J. Milner, D. Carnell, K. Meer, A. Padhani, M. Saunders, P. Hoskin, Phase Ib trial of radiotherapy in combination with combretastatin-A4-phosphate in patients with non-small-cell lung cancer, prostate adenocarcinoma, and squamous cell carcinoma of the head and neck, Ann. Oncol. 1 (2011) 231–237.
[37] S. Sengupta, D. Eavarone, I. Capila, G. Zhao, N. Watson, T. Kiziltepe, R. Sasisekharan, Temporal targeting of tumour cells and neovasculature with a nanoscale delivery system, Nature 436 (2005) 568–572.
[38] G.M. Tozer, V.E. Prise, J. Wilson, M. Cemazar, S. Shan, M.W. Dewhirst, P.R. Barber, B. Vojnovic, D.J. Chaplin, Mechanisms associated with tumor vascular shut-down induced by combretastatin A-4 phosphate: intravital microscopy and measurement of vascular permeability, Cancer Res. 61 (2001) 6413–6422.
[39] L. Zhao, L.M. Ching, P. Kestell, L.R. Kelland, B.C. Baguley, Mechanisms of tumor vascular shutdown induced by 5, 6-dimethylxanthenone-4-acetic acid (DMXAA): increased tumor vascular permeability, Int. J. Cancer 116 (2005) 322–326.
[40] M. Folaron, J. Kalmuk, J. Lockwood, C. Frangou, J. Vokes, S.G. Turowski, M. Merzianu, N.R. Rigual, M. Sullivan-Nasca, M.A. Kuriakose, Vascular priming enhances chemotherapeutic efficacy against head and neck cancer, Oral Oncol. 49 (2013) 893–902.
[41] A.B. Satterlee, J.D. Rojas, P.A. Dayton, L. Huang, Enhancing nanoparticle accumulation and retention in Desmoplastic tumors via vascular disruption for internal radiation therapy, Theranostics 7 (2017) 253–269.
[42] W.J.V. Heeckeren, S.L. Sanborn, A. Narayan, M.M. Cooney, K.R. Mccrae, A.H. Schmaier, et al., Complications from vascular disrupting agents and angiogenesis inhibitors: aberrant control of hemostasis and thrombosis, Curr. Opin. Hematol. 14 (2007) 468–480.
[43] D. Hanahan, J. Folkman, Patterns and emerging mechanisms of the angiogenic switch during tumorigenesis, Cell 86 (1996) 353–364.
[44] D. Hanahan, R.A. Weinberg, The hallmarks of cancer, Cell 100 (2000) 57–70.
[45] D. Hanahan, R.A. Weinberg, Hallmarks of cancer: the next generation, Cell 144 (2011) 646–674.
[46] P.-P. Wong, F. Demircioglu, E. Ghazaly, W. Alrawashdeh, M.R. Stratford, C.L. Scudamore, B. Cereser, T. Crnogorac-Jurcevic, S. McDonald, G. Elia, et al., Dual-action combination therapy enhances angiogenesis while reducing tumor growth and spread, Cancer Cell 27 (2015) 123–137.
[47] R. Neijzen, M.Q. Wong, N. Gill, H. Wang, T. Karim, M. Anantha, D. Strutt, D. Waterhouse, M.B. Bally, I.T. Tai, Irinophore C™, a lipid nanoparticulate formulation of irinotecan, improves vascular function, increases the delivery of sequentially administered 5-FU in HT-29 tumors, and controls tumor growth in patient derived xenografts of colon cancer, J. Control. Release 199 (2015) 72–83.
[48] D. Doleschel, A. Rix, S. Arns, K. Palmowski, F. Gremse, R. Merkle, F. Salopiata, U. Klingmüller, M. Jarsch, F. Kiessling, Erythropoietin improves the accumulation and therapeutic effects of carboplatin by enhancing tumor vascularization and perfusion, Theranostics 5 (2015) 905–918.
[49] E. Bridges, A.L. Harris, Vascular-promoting therapy reduced tumor growth and progression by improving chemotherapy efficacy, Cancer Cell 27 (2015) 7–9.
[50] M.G. Lubner, C.L. Brace, J.L. Hinshaw, F.T. Lee, Microwave tumor ablation: mechanism of action, clinical results, and devices, J. Vasc. Interv. Radiol. 21 (2010) S192–S203.
[51] K. Kurokohchi, S. Watanabe, T. Masaki, N. Hosomi, T. Funaki, K. Arima, S. Yoshida, Y. Miyauchi, S. Kuriyama, Combined use of percutaneous ethanol injection and

radiofrequency ablation for the effective treatment of hepatocelluar carcinoma, Int. J. Oncol. 21 (2002) 841–846.
[52] N.M. Hijnen, E. Heijman, M.O. Köhler, M. Ylihautala, G.J. Ehnholm, A.W. Simonetti, H. Grüll, Tumour hyperthermia and ablation in rats using a clinical MR-HIFU system equipped with a dedicated small animal set-up, Int. J. Hyperth. 28 (2012) 141–155.
[53] Z. Vujaskovic, C. Song, Physiological mechanisms underlying heat-induced radiosensitization, Int. J. Hyperth. 20 (2004) 163–174.
[54] F. Mohamed, P. Marchettini, O.A. Stuart, M. Urano, P.H. Sugarbaker, Thermal enhancement of new chemotherapeutic agents at moderate hyperthermia, Ann. Surg. Oncol. 10 (2003) 463–468.
[55] G. Kong, R.D. Braun, M.W. Dewhirst, Hyperthermia enables tumor-specific nanoparticle delivery: effect of particle size, Cancer Res. 60 (2000) 4440–4445.
[56] G. Kong, R.D. Braun, M.W. Dewhirst, Characterization of the effect of hyperthermia on nanoparticle extravasation from tumor vasculature, Cancer Res. 61 (2001) 3027–3032.
[57] H. Grüll, S. Langereis, Hyperthermia-triggered drug delivery from temperature-sensitive liposomes using MRI-guided high intensity focused ultrasound, J. Control. Release 161 (2012) 317–327.
[58] A.A. Manzoor, L.H. Lindner, C.D. Landon, J.-Y. Park, A.J. Simnick, M.R. Dreher, S. Das, G. Hanna, W. Park, A. Chilkoti, Overcoming limitations in nanoparticle drug delivery: triggered, intravascular release to improve drug penetration into tumors, Cancer Res. 72 (2012) 5566–5575.
[59] A.M. Ponce, B.L. Viglianti, D. Yu, P.S. Yarmolenko, C.R. Michelich, J. Woo, M.B. Bally, M.W. Dewhirst, Magnetic resonance imaging of temperature-sensitive liposome release: drug dose painting and antitumor effects, J. Natl. Cancer Inst. 99 (2007) 53–63.
[60] N. Hijnen, S. Langereis, H. Grüll, Magnetic resonance guided high-intensity focused ultrasound for image-guided temperature-induced drug delivery, Adv. Drug Deliv. Rev. 72 (2014) 65–81.
[61] M. de Smet, E. Heijman, S. Langereis, N.M. Hijnen, H. Grüll, Magnetic resonance imaging of high intensity focused ultrasound mediated drug delivery from temperature-sensitive liposomes: an in vivo proof-of-concept study, J. Control. Release 150 (2011) 102–110.
[62] R.M. Staruch, K. Hynynen, R. Chopra, Hyperthermia-mediated doxorubicin release from thermosensitive liposomes using MR-HIFU: therapeutic effect in rabbit Vx2 tumours, Int. J. Hyperth. 31 (2015) 118–133.
[63] A.J. Gormley, N. Larson, A. Banisadr, R. Robinson, N. Frazier, A. Ray, H. Ghandehari, Plasmonic photothermal therapy increases the tumor mass penetration of HPMA copolymers, J. Control. Release 166 (2013) 130–138.
[64] T.M. Zagar, Z. Vujaskovic, S. Formenti, H. Rugo, F. Muggia, B. O'Connor, R. Myerson, P. Stauffer, I.-C. Hsu, C. Diederich, Two phase I dose-escalation/pharmacokinetics studies of low temperature liposomal doxorubicin (LTLD) and mild local hyperthermia in heavily pretreated patients with local regionally recurrent breast cancer, Int. J. Hyperth. 30 (2014) 285–294.
[65] R. Lencioni, D. Cioni, RFA plus lyso-thermosensitive liposomal doxorubicin: in search of the optimal approach to cure intermediate-size hepatocellular carcinoma, Hepatic Oncol. 3 (2016) 193–200.
[66] H.C. Schwickert, M. Stiskal, T. Roberts, C. Van Dijke, J. Mann, A. Mühler, D.M. Shames, F. Demsar, A. Disston, R.C. Brasch, Contrast-enhanced MR imaging assessment of tumor capillary permeability: effect of irradiation on delivery of chemotherapy, Radiology 198 (1996) 893–898.
[67] T. Lammers, V. Subr, P. Peschke, R. Kühnlein, W. Hennink, K. Ulbrich, F. Kiessling, M. Heilmann, J. Debus, P. Huber, Image-guided and passively tumour-targeted polymeric nanomedicines for radiochemotherapy, Br. J. Cancer 99 (2008) 900–910.
[68] C.d.L. Davies, L.M. Lundstrøm, J. Frengen, L. Eikenes, Ø.S. Bruland, O. Kaalhus, M.H. Hjelstuen, C. Brekken, Radiation improves the distribution and uptake of liposomal doxorubicin (caelyx) in human osteosarcoma xenografts, Cancer Res. 64 (2004) 547–553.
[69] A.G. Koukourakis, Sofia Koukouraki, Stelios Kakolyris, Vassilis Georgoulias, Antigoni Velidaki, Spyridon Archimandritis, M.I. Nikolaos N. Karkavitsas, High intratumoral accumulation of stealth liposomal doxorubicin in sarcomas: rationale for combination with radiotherapy, Acta Oncol. 39 (2000) 207–211.
[70] M. Machtay, J. Moughan, A. Trotti, A.S. Garden, R.S. Weber, J.S. Cooper, A. Forastiere, K.K. Ang, Factors associated with severe late toxicity after concurrent chemoradiation for locally advanced head and neck cancer: an RTOG analysis, J. Clin. Oncol. 26 (2008) 3582–3589.
[71] G. Calais, M. Alfonsi, E. Bardet, C. Sire, T. Germain, P. Bergerot, B. Rhein, J. Tortochaux, P. Oudinot, P. Bertrand, Randomized trial of radiation therapy versus concomitant chemotherapy and radiation therapy for advanced-stage oropharynx carcinoma, J. Natl. Cancer Inst. 91 (1999) 2081–2086.
[72] N.J. Nonzee, N.A. Dandade, T. Markossian, M. Agulnik, A. Argiris, J.D. Patel, R.C. Kern, H.G. Munshi, E.A. Calhoun, C.L. Bennett, Evaluating the supportive care costs of severe radiochemotherapy-induced mucositis and pharyngitis, Cancer 113 (2008) 1446–1452.
[73] D.-X. Qin, R. Zheng, J. Tang, J.-X. Li, Y.-H. Hu, Influence of radiation on the blood-brain barrier and optimum time of chemotherapy, Int. J. Radiat. Oncol. Biol. Phys. 19 (1990) 1507–1510.
[74] D. Qin, G. Ou, H. Mo, Y. Song, G. Kang, Y. Hu, X. Gu, Improved efficacy of chemotherapy for glioblastoma by radiation-induced opening of blood-brain barrier: clinical results, Int. J. Radiat. Oncol. Biol. Phys. 51 (2001) 959–962.
[75] I. Lentacker, I. De Cock, R. Deckers, S. De Smedt, C. Moonen, Understanding ultrasound induced sonoporation: definitions and underlying mechanisms, Adv. Drug Deliv. Rev. 72 (2014) 49–64.
[76] S. Bao, B.D. Thrall, D.L. Miller, Transfection of a reporter plasmid into cultured cells by sonoporation in vitro, Ultrasound Med. Biol. 23 (1997) 953–959.
[77] D.L. Miller, S.V. Pislaru, J.F. Greenleaf, Sonoporation: mechanical DNA delivery by ultrasonic cavitation, Somat. Cell Mol. Genet. 27 (2002) 115–134.
[78] A. Dasgupta, M. Liu, T. Ojha, G. Storm, F. Kiessling, T. Lammers, Ultrasound-mediated drug delivery to the brain: principles, progress and prospects, Drug Discov. Today Technol. 20 (2016) 41–48.
[79] K. Hynynen, N. McDannold, N. Vykhodtseva, F.A. Jolesz, Noninvasive MR imaging–guided focal opening of the blood-brain barrier in rabbits 1, Radiology 220 (2001) 640–646.
[80] M. Kinoshita, N. McDannold, F.A. Jolesz, K. Hynynen, Noninvasive localized delivery of Herceptin to the mouse brain by MRI-guided focused ultrasound-induced blood–brain barrier disruption, Proc. Natl. Acad. Sci. 103 (2006) 11719–11723.
[81] M. Aryal, N. Vykhodtseva, Y.-Z. Zhang, N. McDannold, Multiple sessions of liposomal doxorubicin delivery via focused ultrasound mediated blood–brain barrier disruption: a safety study, J. Control. Release 204 (2015) 60–69.
[82] T. Lammers, P. Koczera, S. Fokong, F. Gremse, J. Ehling, M. Vogt, A. Pich, G. Storm, M. Van Zandvoort, F. Kiessling, Theranostic USPIO-loaded microbubbles for mediating and monitoring blood-brain barrier permeation, Adv. Funct. Mater. 25 (2015) 36–43.
[83] H.-L. Liu, M.-Y. Hua, P.-Y. Chen, P.-C. Chu, C.-H. Pan, H.-W. Yang, C.-Y. Huang, J.-J. Wang, T.-C. Yen, K.-C. Wei, Blood-brain barrier disruption with focused ultrasound enhances delivery of chemotherapeutic drugs for glioblastoma treatment 1, Radiology 255 (2010) 415–425.
[84] N. McDannold, C.D. Arvanitis, N. Vykhodtseva, M.S. Livingstone, Temporary disruption of the blood–brain barrier by use of ultrasound and microbubbles: safety and efficacy evaluation in rhesus macaques, Cancer Res. 72 (2012) 3652–3663.
[85] N. Radovini, World First: Blood–Brain Barrier Opened non-invasively to Deliver Chemotherapy, Sunnybrook Hospital, Sunnybrook Canada: Press Release, 2015.
[86] A. Carpentier, M. Canney, A. Vignot, V. Reina, K. Beccaria, C. Horodyckid, et al., Clinical trial of blood-brain barrier disruption by pulsed ultrasound, Sci. Transl. Med. 8 (2016) 343RE2.
[87] B. Theek, M. Baues, T. Ojha, D. Möckel, S.K. Veettil, J. Steitz, L. van Bloois, G. Storm, F. Kiessling, T. Lammers, Sonoporation enhances liposome accumulation and penetration in tumors with low EPR, J. Control. Release 231 (2016) 77–85.
[88] G. Dimcevski, S. Kotopoulis, T. Bjånes, D. Hoem, J. Schjøtt, B.T. Gjertsen, M. Biermann, A. Molven, H. Sorbye, E. McCormack, A human clinical trial using ultrasound and microbubbles to enhance gemcitabine treatment of inoperable pancreatic cancer, J. Control. Release 243 (2016) 172–181.
[89] T.J. Dougherty, C.J. Gomer, B.W. Henderson, G. Jori, D. Kessel, M. Korbelik, J. Moan, Q. Peng, Photodynamic therapy, J. Natl. Cancer Inst. 90 (1998) 889–905.
[90] B.W. Henderson, T.J. Dougherty, How does photodynamic therapy work? Photochem. Photobiol. 55 (1992) 145–157.
[91] V.H. Fingar, T.J. Wieman, S.A. Wiehle, P.B. Cerrito, The role of microvascular damage in photodynamic therapy: the effect of treatment on vessel constriction, permeability, and leukocyte adhesion, Cancer Res. 52 (1992) 4914–4921.
[92] W.G. Roberts, T. Hasan, Role of neovasculature and vascular permeability on the tumor retention of photodynamic agents, Cancer Res. 52 (1992) 924–930.
[93] B. Chen, B.W. Pogue, J.M. Luna, R.L. Hardman, P.J. Hoopes, T. Hasan, Tumor vascular permeabilization by vascular-targeting photosensitization: effects, mechanism, and therapeutic implications, Clin. Cancer Res. 12 (2006) 917–923.
[94] L.A. Sporn, T.H. Foster, Photofrin and light induces microtubule depolymerization in cultured human endothelial cells, Cancer Res. 52 (1992) 3443–3448.
[95] J.W. Snyder, W.R. Greco, D.A. Bellnier, L. Vaughan, B.W. Henderson, Photodynamic therapy, Cancer Res. 63 (2003) 8126–8131.
[96] Z. Zhen, W. Tang, Y.-J. Chuang, T. Todd, W. Zhang, X. Lin, G. Niu, G. Liu, L. Wang, Z. Pan, Tumor vasculature targeted photodynamic therapy for enhanced delivery of nanoparticles, ACS Nano 8 (2014) 6004–6013.
[97] W. Gao, Z. Wang, L. Lv, D. Yin, D. Chen, Z. Han, Y. Ma, M. Zhang, M. Yang, Y. Gu, Photodynamic therapy induced enhancement of tumor vasculature permeability using an upconversion nanoconstruct for improved intratumoral nanoparticle delivery in deep tissues, Theranostics 6 (2016) 1131–1144.
[98] M. Mitsunaga, M. Ogawa, N. Kosaka, L.T. Rosenblum, P.L. Choyke, H. Kobayashi, Cancer cell-selective in vivo near infrared photoimmunotherapy targeting specific membrane molecules, Nat. Med. 17 (2011) 1685–1691.
[99] H. Kobayashi, R. Watanabe, P.L. Choyke, Improving conventional enhanced permeability and retention (EPR) effects; what is the appropriate target, Theranostics 4 (2013) 81–89.
[100] K. Sano, T. Nakajima, P.L. Choyke, H. Kobayashi, Markedly enhanced permeability and retention effects induced by photo-immunotherapy of tumors, ACS Nano 7 (2012) 717–724.
[101] F. Ogata, T. Nagaya, Y. Nakamura, K. Sato, S. Okuyama, Y. Maruoka, et al., Near-infrared photoimmunotherapy: a comparison of light dosing schedules, Oncotarget 8 (2017) 35069–35075.
[102] M.O. Leach, K. Brindle, J. Evelhoch, J.R. Griffiths, M.R. Horsman, A. Jackson, G.C. Jayson, I.R. Judson, M. Knopp, R.J. Maxwell, The assessment of antiangiogenic and antivascular therapies in early-stage clinical trials using magnetic resonance imaging: issues and recommendations, Br. J. Cancer 92 (2005) 1599–1610.
[103] S. Kunjachan, J. Ehling, G. Storm, F. Kiessling, T. Lammers, Noninvasive imaging of nanomedicines and nanotheranostics: principles, progress, and prospects, Chem. Rev. 115 (2015) 10907–10937.
[104] T. Ojha, L. Rizzo, G. Storm, F. Kiessling, T. Lammers, Image-guided drug delivery: preclinical applications and clinical translation, Expert Opin. Drug Deliv. 8 (2015) 1203–1207.